Main Results of *PRD108 (2023) L111103* [BABAR]and *arXiv:2312.02053* [Davier-Hoecker-Lutz-Malaescu-Zhang]

Outline

- Introduction
- Publication 1
- Publication 2
- Summary

PRD108 (2023) L111103: Study of additional radiation in the initial-state-radiation (ISR) processes $e^+e^-\to\mu^+\mu^-\gamma$ and $e^+e^-\to\pi^+\pi^-\gamma$ in the BABAR experiment
arXiv:2312.02053: Tensions in $e^+e^-\to\pi^+\pi^-(\gamma)$ measurements: the new landscape of data-driven hadronic vacuum polarisation (HVP) predictions for the muon g-2

Introduction - Anomalous Magnetic Moment

➢ Lepton magnetic moment:

$$\vec{\mu}_\ell = g_\ell \frac{e}{2m_\ell} \vec{s}_\ell$$

➢ The anomalous magnetic moment:

$$a_\ell = \frac{g_\ell - 2}{2} \qquad = 0.00116\ldots$$

➢ It is one of the most precise observables measured and predicted in particle physics of the Standard Model

Introduction – Measurements vs Predictions

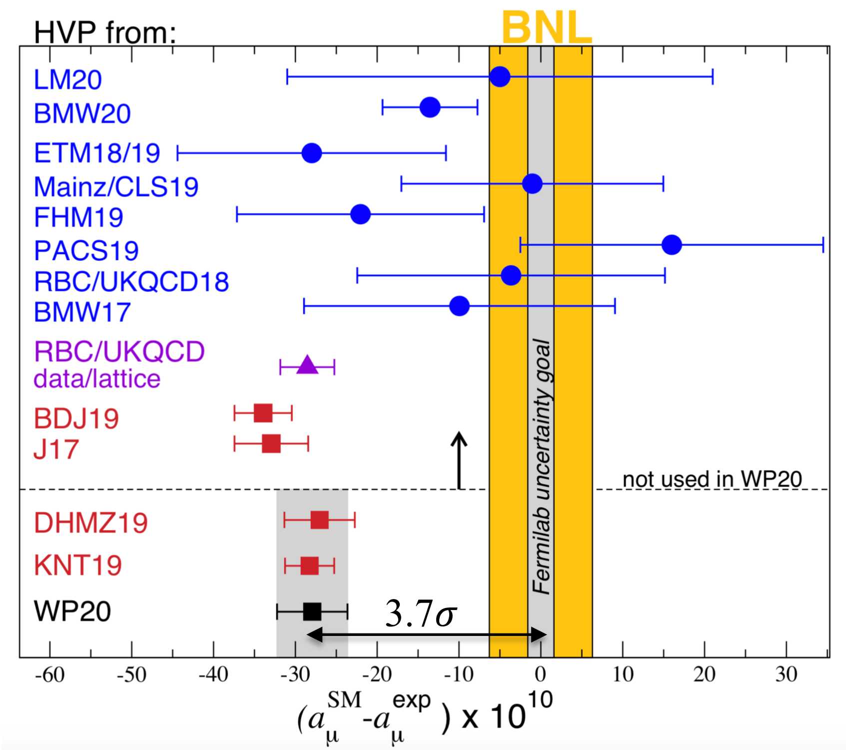

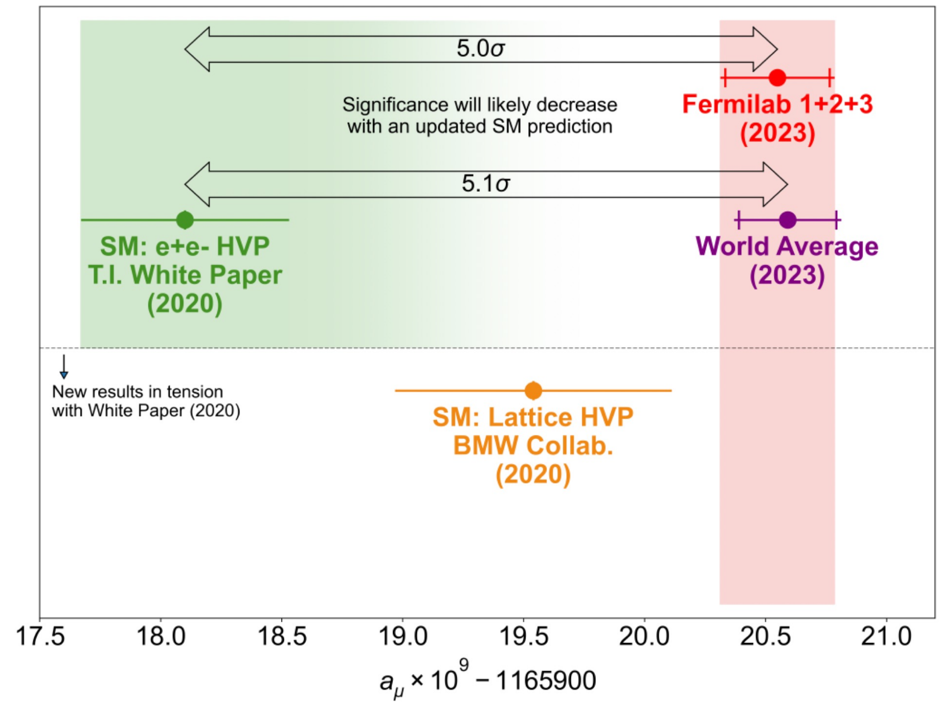

- Longstanding discrepancy between dispersion-relation-based prediction and the measurements
- New Fermilab measurements now more precise than predictions (another factor of 2 by 2025)
- Lattice HVP less precise than dispersion-relation-based prediction but in disagreement

WP20 = White Paper 2020 [Phys. Rept. 887 (2020) 1] from the Muon g-2 Theory Initiative group
DHMZ19 = Davier-Hoecker-Malaescu-Zhang [Eur. Phys. J. C 80 (2020) 241] > 600 citations

Introduction - Theoretical Contributions

$$a_\mu^{\rm th} = a_\mu^{\rm SM} + a_\mu^{\rm BSM}$$

$$a_\mu^{\rm SM} = a_\mu^{\rm QED} + a_\mu^{\rm had} + a_\mu^{\rm Weak}$$

$$a_\mu^{\rm BSM}$$

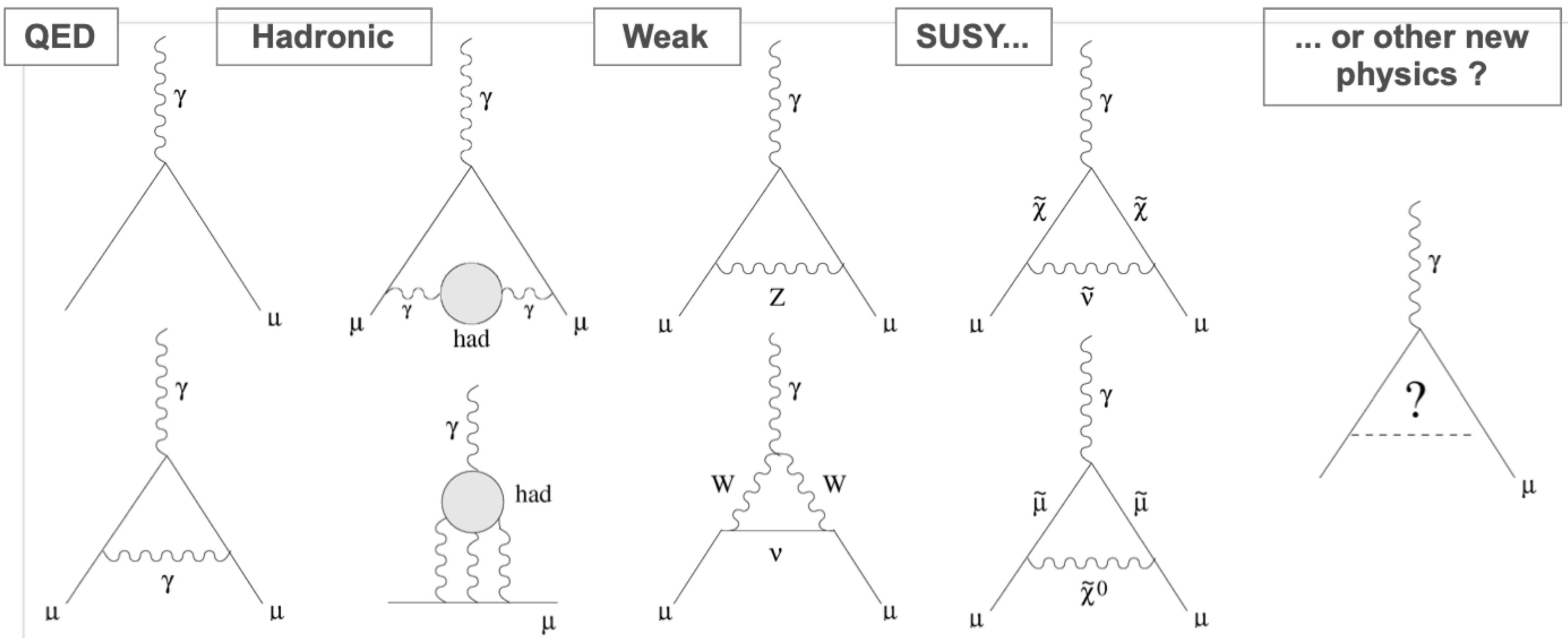

Introduction - Dispersion Relation

$$a_\mu^{\text{had}} = a_\mu^{\text{had,LO}} + a_\mu^{\text{had,HO}} + a_\mu^{\text{had,LBL}}$$

Based on analyticity and unitarity, the LO HVP contribution can be calculated using the dispersion relation [1] over $e^+e^- \to$ hadrons cross sections

$$a_\mu^{\text{had,LO}} = \frac{\alpha^2}{3\pi^2}\int_{4m_\pi^2}^{\infty} ds \frac{K(s)}{s} R(s)$$

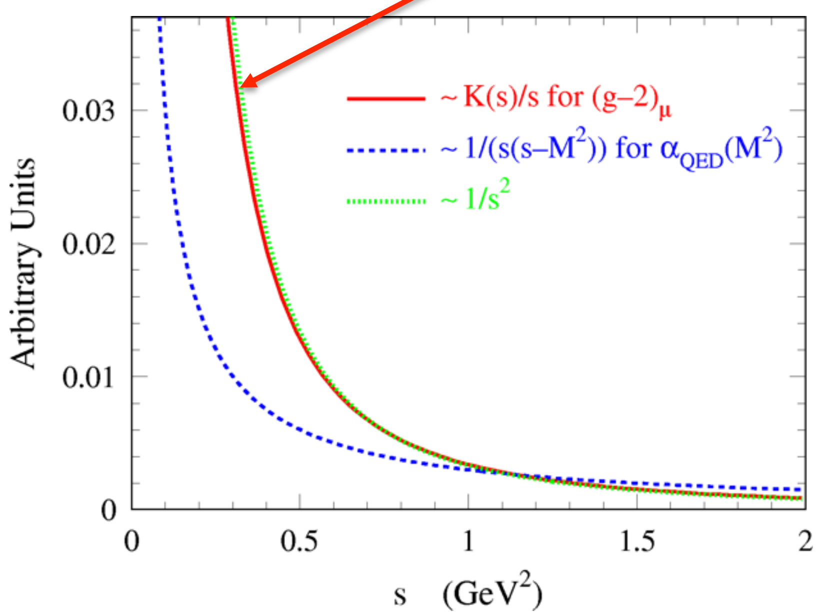

Born: $\sigma^{(0)}(s) = \sigma(s)\left(\alpha / \alpha(s)\right)^2$

$$12\pi \, \text{Im}\Pi_\gamma(s) = \frac{\sigma^0 \left[e^+e^- \to \text{hadrons}\,(\gamma_{FSR})\right]}{\sigma_{pt}} \equiv R(s)$$

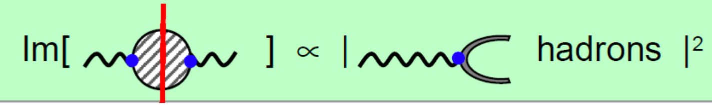

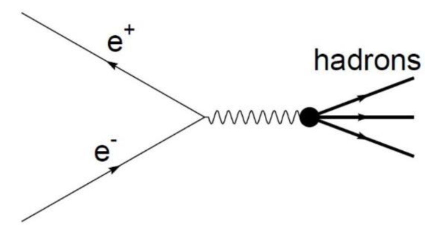

The QED kernel K(s) [2] has such an s dependence that low energy data contribute most:

$e^+e^- \to \pi^+\pi^-$ contributes ~73% (58% in uncertainty)

[1] Bouchiat and Michel, 1961
[2] Brodsky, de Rafael, 1968

Introduction: Different Contributing Channels

Figure 21(a) from arXiv:1802.02995

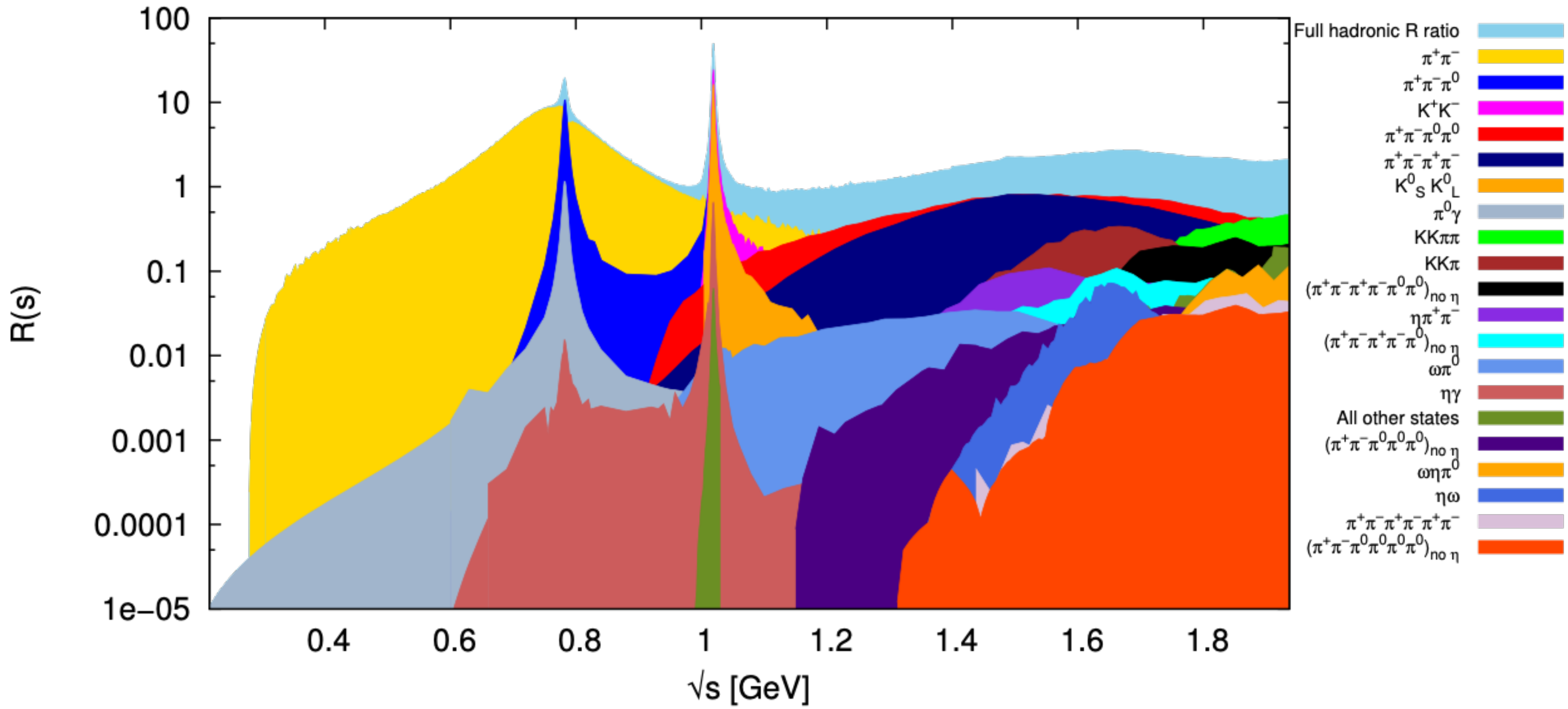

$\pi\pi$ is the dominant channel (at low energy) for the LO HVP contribution

Introduction - Discrepancy among $\pi\pi$ Measurements

Plots from publication 2 (arXiv:2312.02053)

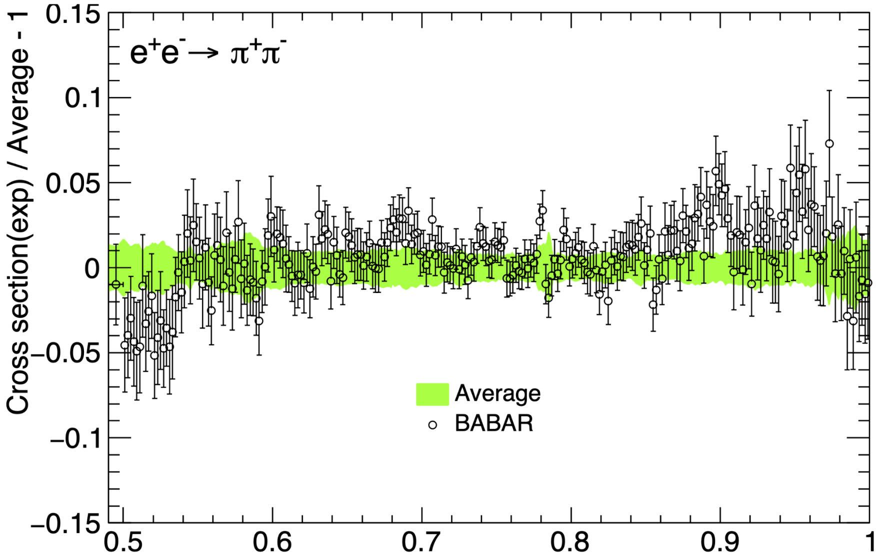

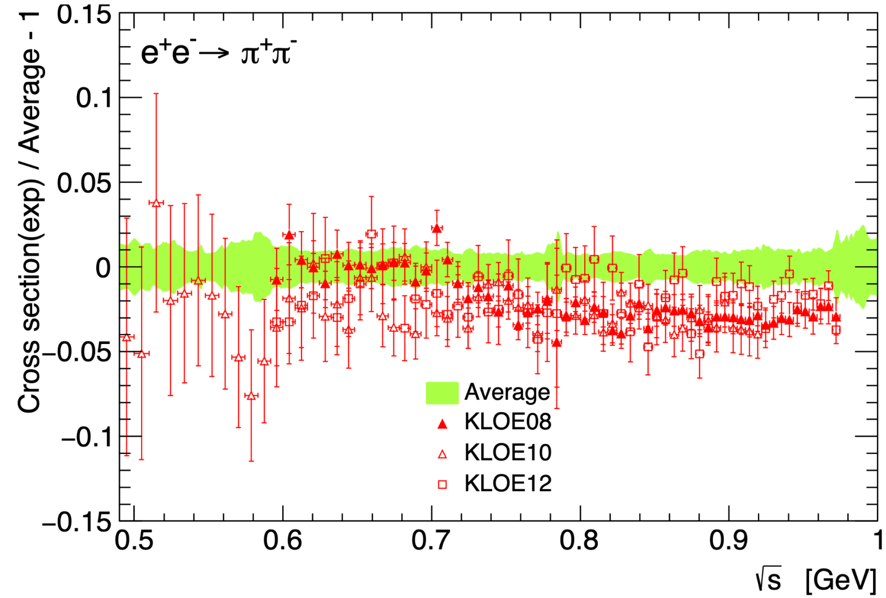

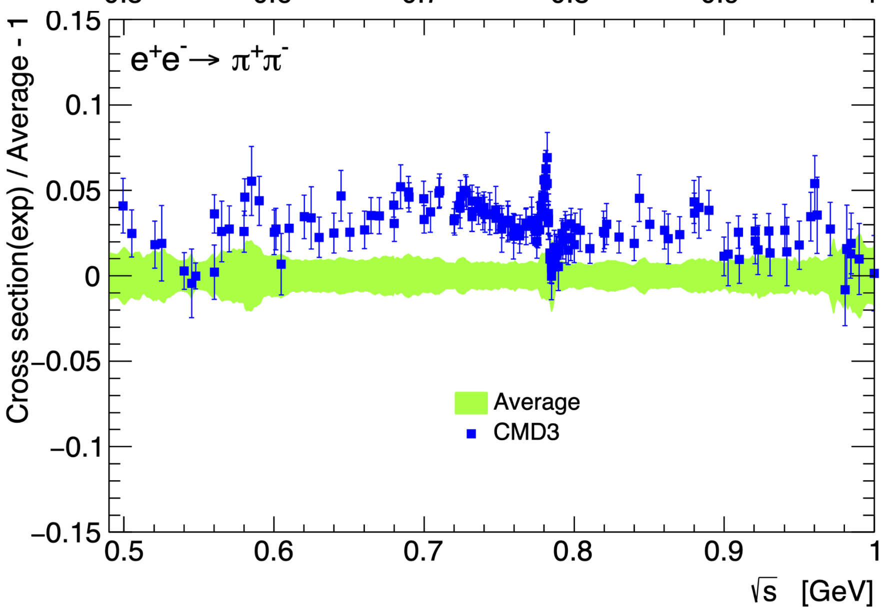

- Green band correspond to our combination
- Using a dedicated package HVPTools
- BABAR, KLOE and CMD-3 disagree in the dominant ρ peak region

Introduction - Use of Tau Data from $\pi\pi^0$ Channel

Fig 4(d) from DHMYZ (EPJC74(2014)2803)

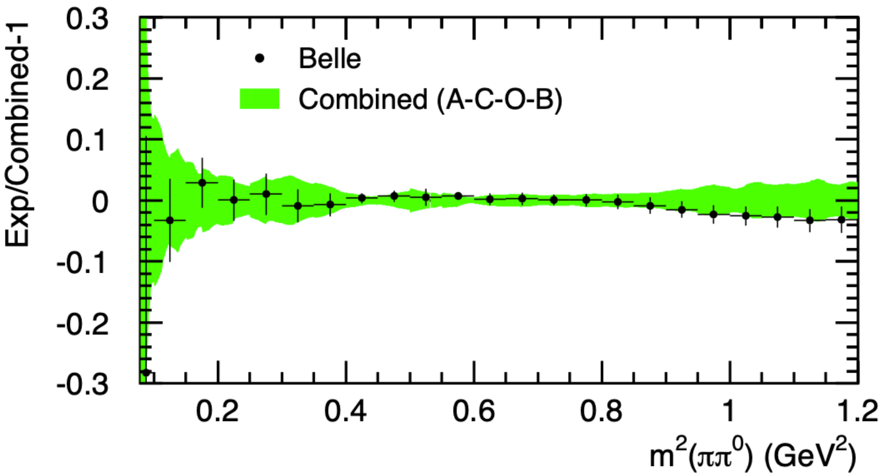

Fig 5 from DHMYZ (EPJC66(2010)1)

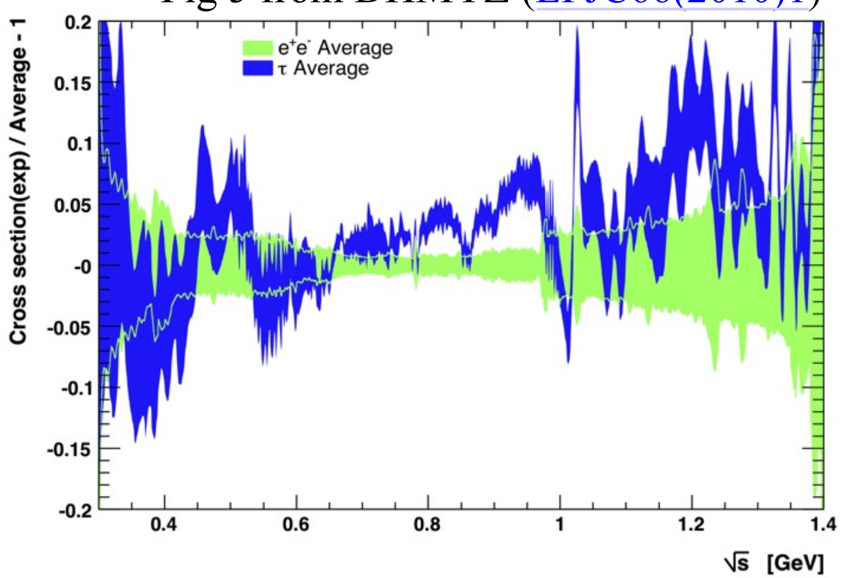

$\pi\pi$ cross section is $\propto$ its spectral function v:

$$\sigma(e^+e^- \to \pi^+\pi^-) = \frac{4\pi\alpha^2}{s} v_0(s)$$

v can be expressed as its form factor F:

$$v_0(s) = \frac{\beta_0^3(s)}{12} |F_\pi^0(s)|^2$$

Similarly for tau decay in $\pi\pi^0$ channel:

$$v_-(s) = \frac{\beta_-^3(s)}{12} |F_\pi^-(s)|^2$$

So tau data can be used once the isospin corrections are taken into account

Motivations for the new $\pi\pi$ BABAR Analysis

Use full BABAR data sample 424 fb^{-1} on $\Upsilon(4S)$ and 44 fb^{-1} off-peak (instead of 232 fb^{-1} for the previous BABAR measurement in 2009)

The previous analysis used particle identification (PID) for selecting $\pi\pi$ and $\mu\mu$ channels. The track momenta were limited above 1 GeV/c (a big loss of the stat)

The new analysis will use kinematic distributions (different spins) to separate $\pi\pi$ and $\mu\mu$ for transverse momenta down to 0.1 GeV/c

➔ A gain of a factor of 7 in statistics
➔ Remove the dominant systematic uncertainty from PID

The publication PRD108 (2023) L111103 (the thesis work of Dongyun BAI, studying events with one or two hard photons in additional to the ISR photon) is an important step towards the final BABAR cross-section measurements in $\pi\pi$ and $\mu\mu$ channels

Introduction to PRD108 (2023) L111103

Lowest-order (LO) ISR (initial-state-radiation)

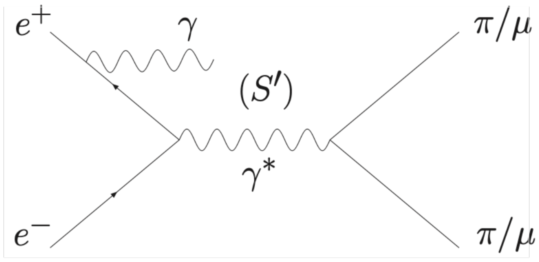

Lowest-order (LO) FSR (final-state-radiation)

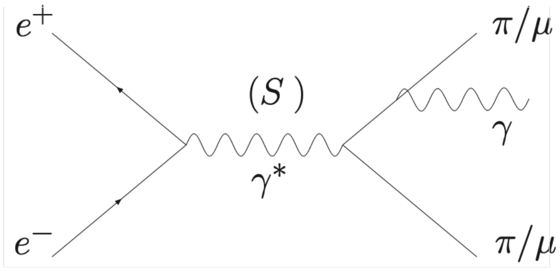

Next-to-leading-order (NLO) ISR

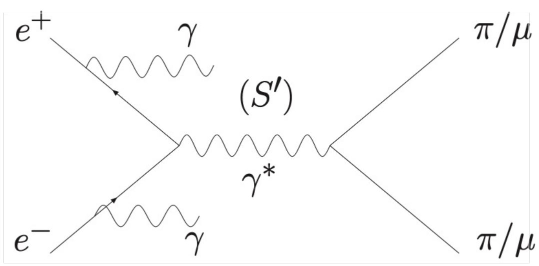

Next-to-leading-order (NLO) FSR

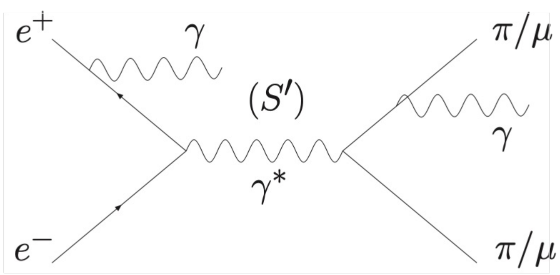

- Events with NLO soft photon radiation & virtual loop (not shown) are LO like
- We study events with 2 (NLO) and 3 (NNLO) hard-photon radiation ($E_\gamma > 100-200$ MeV in CM (center-of-mass) or lab frame) in this analysis

Overview of the kinematic fits

- ➢ NLO fits
  - ➢ Small Angle (SA) fit
  - ➢ Large Angle (LA) fit

NLO

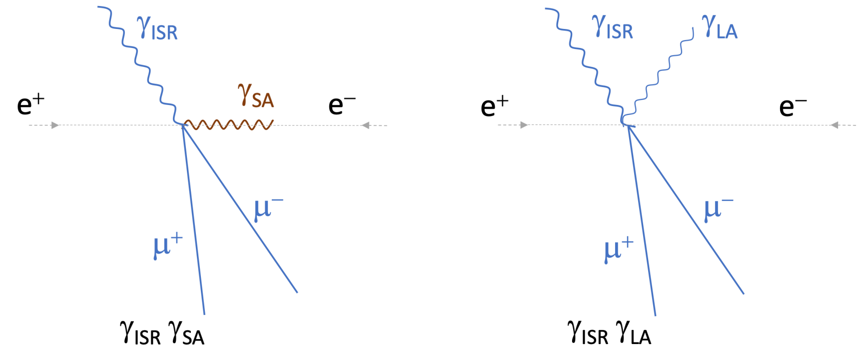

- ➢ NNLO fits
  - ➢ 2SA fit results
  - ➢ SA+LA fit results
  - ➢ 2LA fit results

NNLO

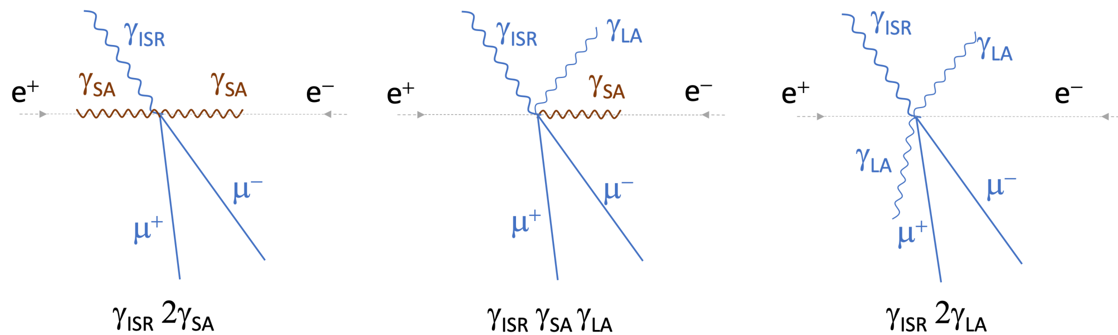

In all fits, only photons with $E_\gamma > 50$ MeV considered

Data / MC Samples

- Data: Runs 1-6 [full data sample @Υ(4S)]
  - 424.2 fb^{-1} [@Υ(4S)], 43.9 fb^{-1} [below Υ(4S)]

- MC signal ($\mu\mu\gamma$, $\pi\pi\gamma$) samples
  - Phokhara9.1 NLO (10 times data stat)
  - AfkQED up to NNLO ($\lesssim$ 1/2 data stat)
    - A minimum mass $m_{X\gamma} > 8$ GeV/c^2 ➜ $E^*_{add.\gamma} < 2.3$ GeV
    - NLO/NNLO ISR collinear to beams and/or FSR

- MC background samples
  - Phokhara9.1: $KK\gamma$
  - AfkQED: $e^+e^-\to(\pi^+\pi^-\pi^0, \pi^+\pi^-2\pi^0, \ldots)\gamma$
  - JETSET: $e^+e^-\to q q$bar ($q=u,d,s,c$)
  - Koralb: $e^+e^-\to\tau^+\tau^-$
  - All backgrounds are normalized using measured cross sections by BABAR except for $3\pi\gamma$, qqbar where dedicated studies performed

Event Selection

- Follow closely previous analyses but looser in track momentum (p >1 GeV/c requirement removed)

- Two tracks with opposite charges, each with
  - θ: 0.4−2.45 rad
  - $p_T > 0.1$ GeV/c
  - at least 15 hits in DCH
  - $doca_{xy} < 5$mm
  - $|\Delta_z| < 6$ cm
  - PID applied, but using π mass hypothesis for invariant mass $\pi\pi$ or $\mu\mu$

- ISR photon candidate:
  - θ: 0.35−2.4 rad
  - $E^* > 4$ GeV
  - If more than one detected photon, take the one having the largest E*

- Allowing additional tracks and photons not satisfying the above requirements in a given event

NLO Fits with 2 Hard Photons

- Two NLO fits
  - $\gamma_{ISR}\gamma_{LA}$: for each additional LA γ with θ_γ: 0.35−2.4 rad, the one with lowest χ^2 is retained
  - $\gamma_{ISR}\gamma_{SA}$: a SA γ is approximated as being collinear with one of the beams (ignoring additional detected photons)
- Both fits use the measured ISR energy and direction, momenta and angles of two tracks
- Pipi processes have much larger background than dimuon processes, largely suppressed by BDT-based 2D-χ^2 optimized selection
  - Signal efficiency 98-99%
- NLO LA sample: $\chi^2_{LA} < \chi^2_{SA}$, $E_\gamma > 200$ MeV
- NLO SA sample: $\chi^2_{SA} < \chi^2_{LA}$, $E^*_{\gamma SA} > 200$ MeV
- LO sample: events below the thresholds

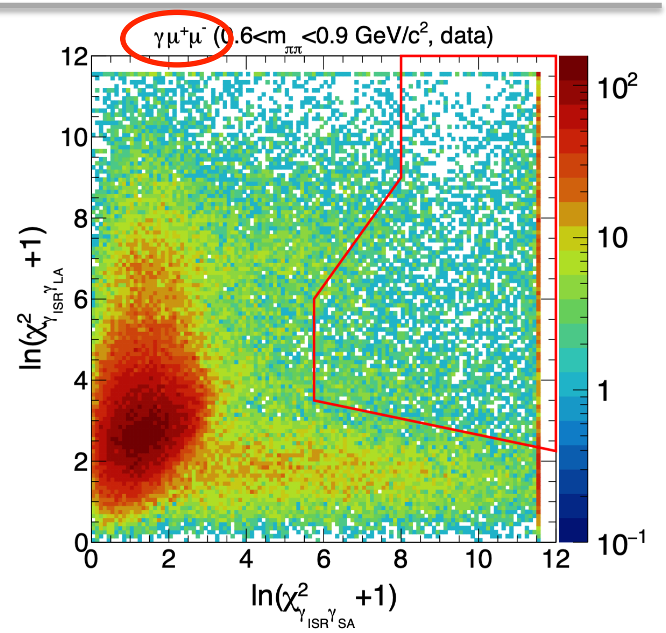

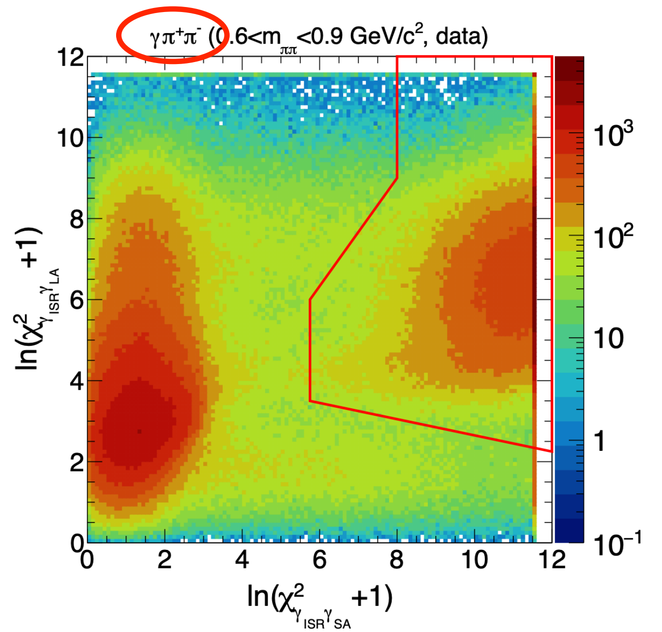

NLO LA Fit Results (E_γ > 200 MeV)

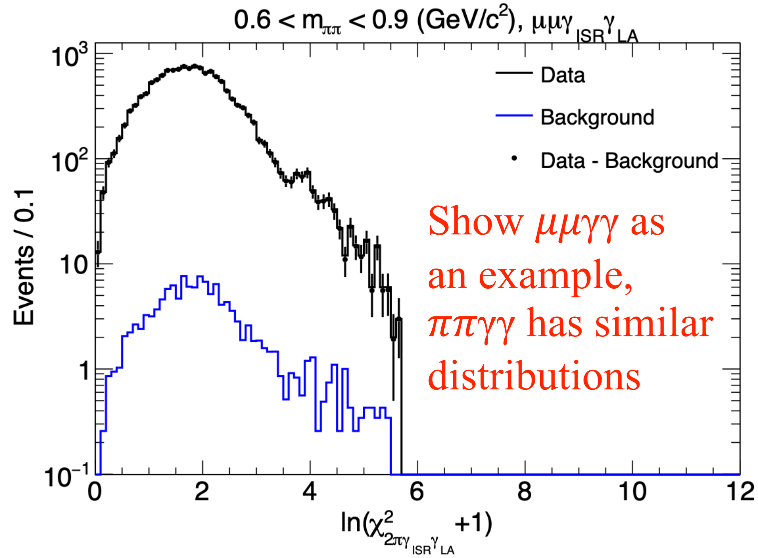

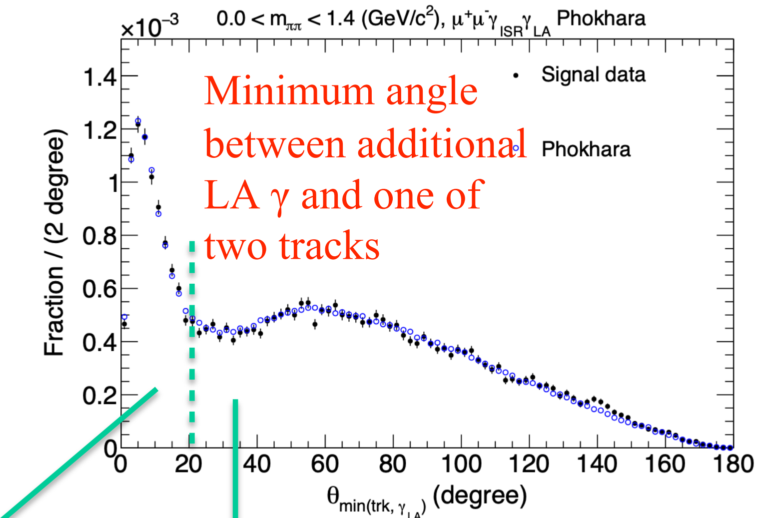

Fraction in data = event-yield of one fit category over those of all categories

Here, MC distributions normalized to data one

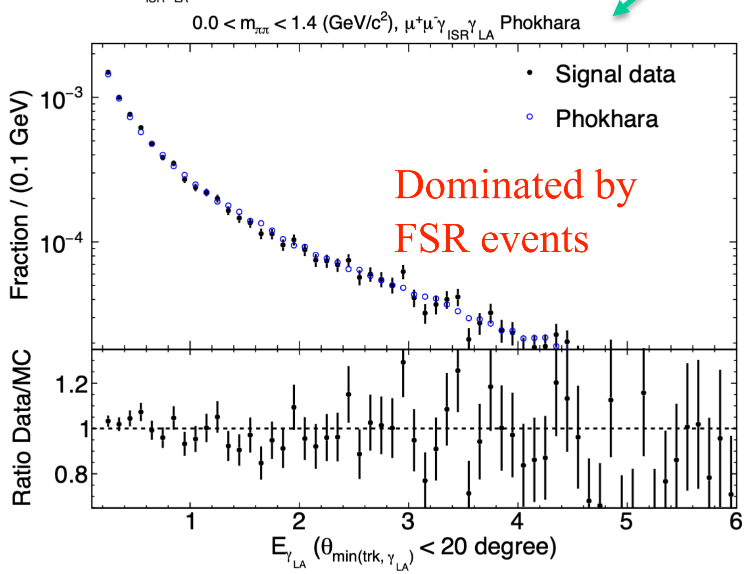

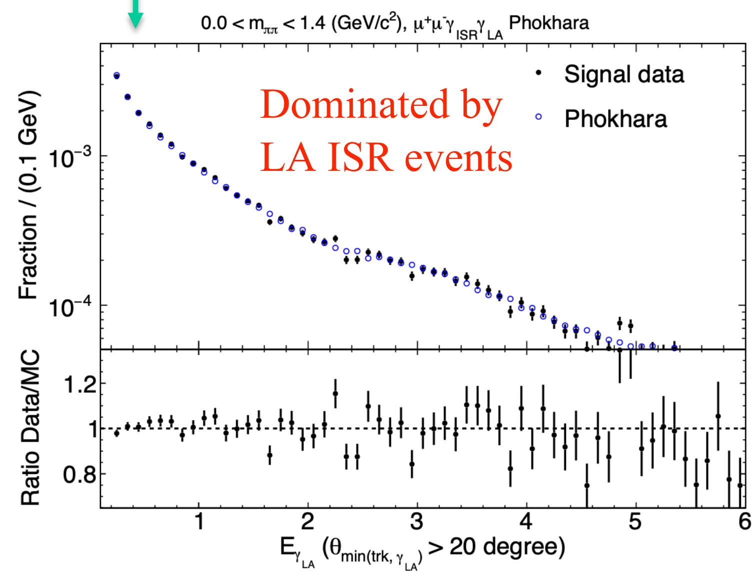

Good agreement data/Phokhara in shape for the angular and energy distributions

NLO SA Fit Results ($E^*_{\gamma SA}$>200 MeV)

μμγγ process

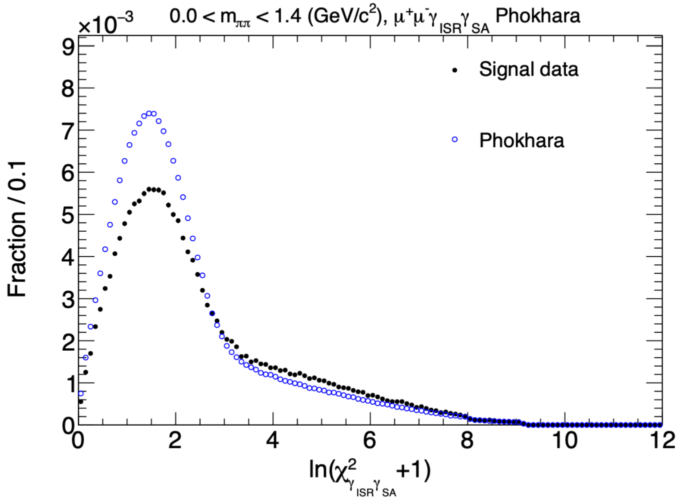

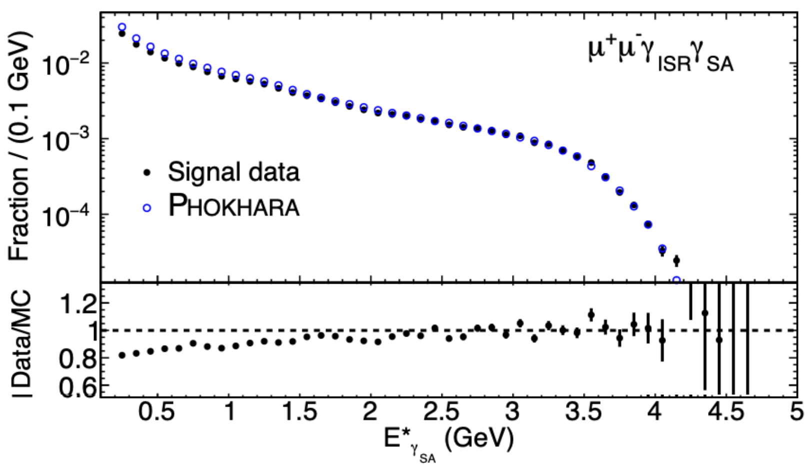

ππγγ process

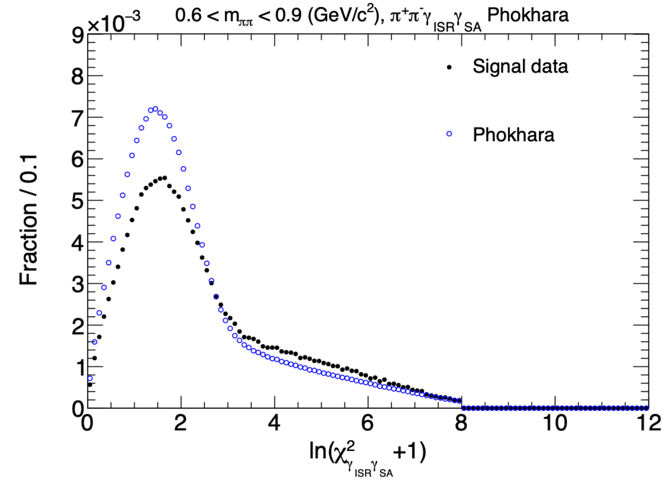

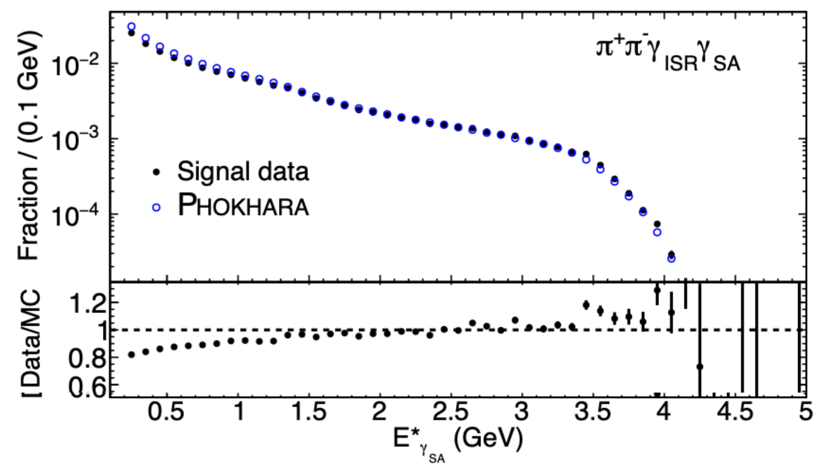

χ^2 distributions: both (*μμ* & *ππ*) show a long tail
$E^*_{\gamma SA}$ data/Phokhara: both show deficit & a slope

Bias of the collinear approximation studied (backup)

Further NLO Study w/o Collinear Approximation

Zero constraint (0C) calculation:

- ➢ Use 4-momenta of the beams and of the two charged particles, and the angles of the main ISR photon + energy and momentum conservation relations, it is possible to calculate 4 unknowns:
  - the energy and angles of the additional γ
  - the energy of the main ISR γ
- ➢ Need to suppress spurious photons when they are aligned with the main ISR γ

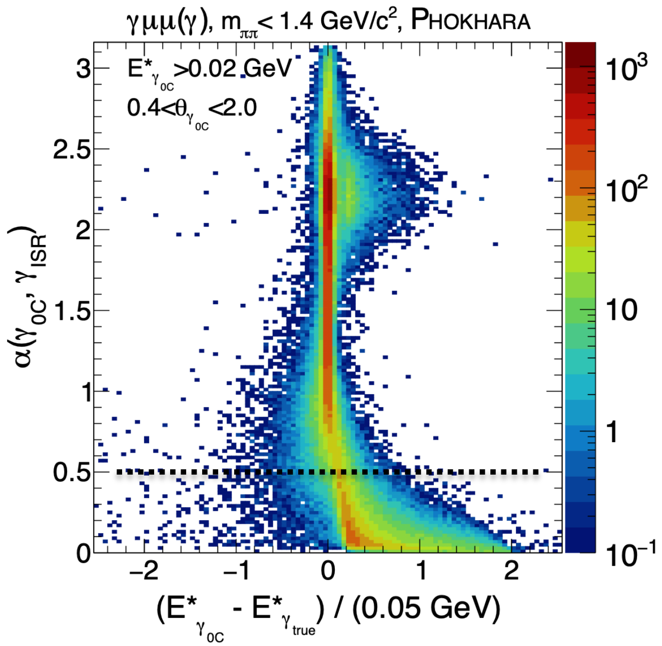

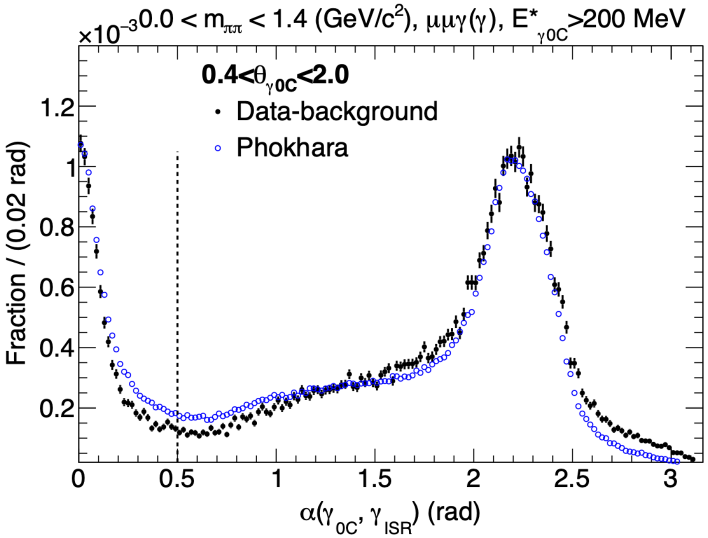

Events with $\alpha(\gamma_{0C}, \gamma_{ISR}) < 0.5$ rejected for the 0C study

NLO 0C Results

Calculated polar angle $\theta_{\gamma 0C}$ distribution
($E^*_{\gamma 0C} > 200$ MeV)

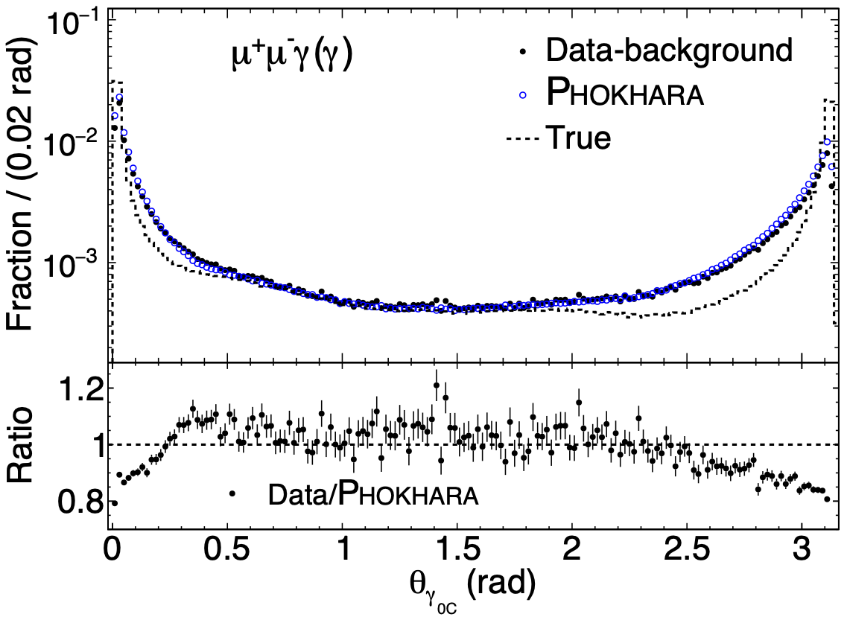

Phokhara NLO SA γ rate > data
Phokhara NLO LA γ rate ~ data
(the slight LA excess in data is due to larger resolution tails)

Calculated energy $E^*_{\gamma 0C}$ distribution

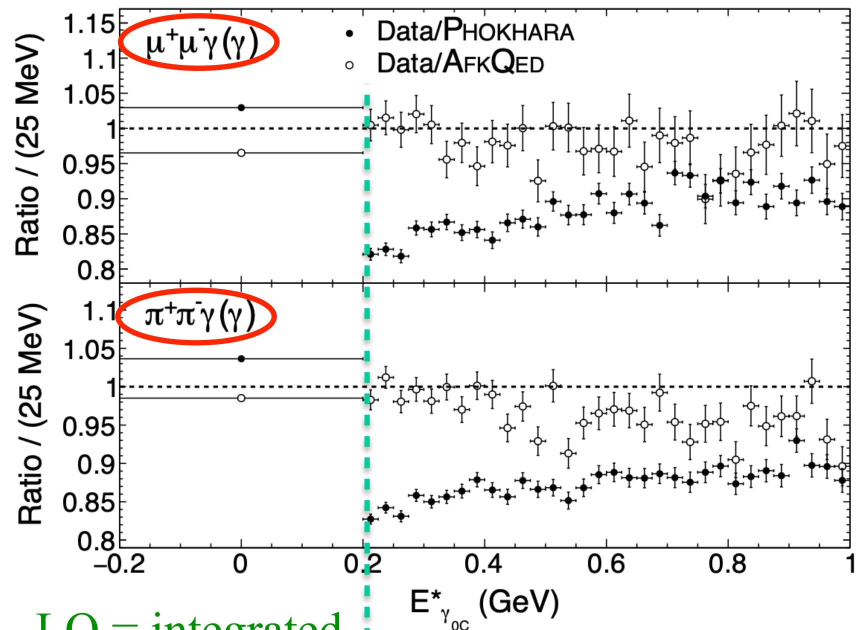

LO = integrated events < 0.2 GeV

NLO

Data/Phokhara Mismatch LO-NLO,
NLO slope ~ NLO SA fit
Data/AfkQED similar rate LO & NLO

NNLO Fits with 3 Hard Photons

- Three NNLO fits
  - $\gamma_{ISR}2\gamma_{SA}$: the energies of two additional SA photons are fitted, each approximated to be collinear with one of the beams
  - $\gamma_{ISR}\gamma_{SA}\gamma_{LA}$: one additional LA photon is measured in the detector and one SA photon is approximated to be collinear with one of the beams, which provides the best fit.
  - $\gamma_{ISR}2\gamma_{LA}$: two additional LA photons are measured in the detector. The fit with lowest χ^2 among all combinations of the two photons is retained.

- While all events are submitted to the $\gamma_{ISR}2\gamma_{SA}$ fit, only events with at least one or two additional detected photons enter the $\gamma_{ISR}\gamma_{SA}\gamma_{LA}$ and $\gamma_{ISR}2\gamma_{LA}$ fits, respectively. Events of the $\gamma_{ISR}2\gamma_{LA}$ category are not simulated by either generator (so no efficiency correction is possible)

- Each NNLO fit category is selected by requiring the corresponding fit has the best χ^2 over all fits of other categories

- Two types of background
  - NLO feed-through estimated by Phokhara
  - Other background

NNLO 2SA Fit Results ($E^*\gamma_{SA1} > 200$ MeV, $E^*\gamma_{SA2} > 100$ MeV)

$\mu\mu\gamma\gamma\gamma$ process

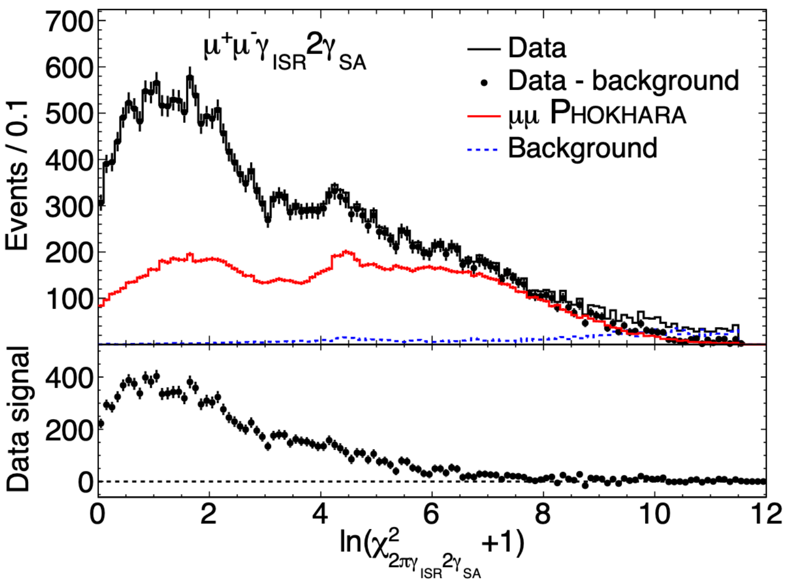

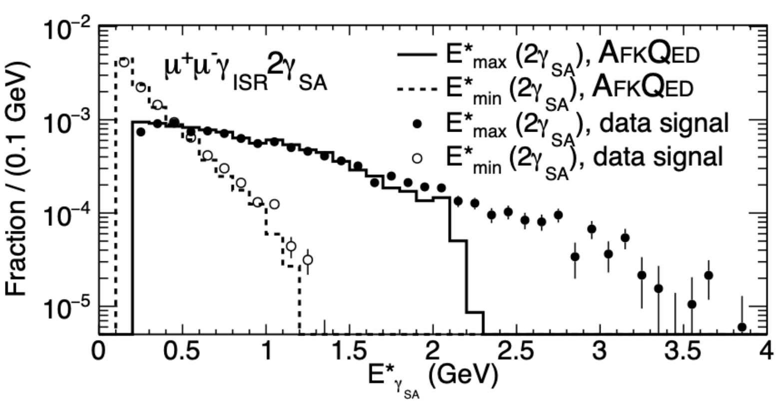

$\pi\pi\gamma\gamma\gamma$ process

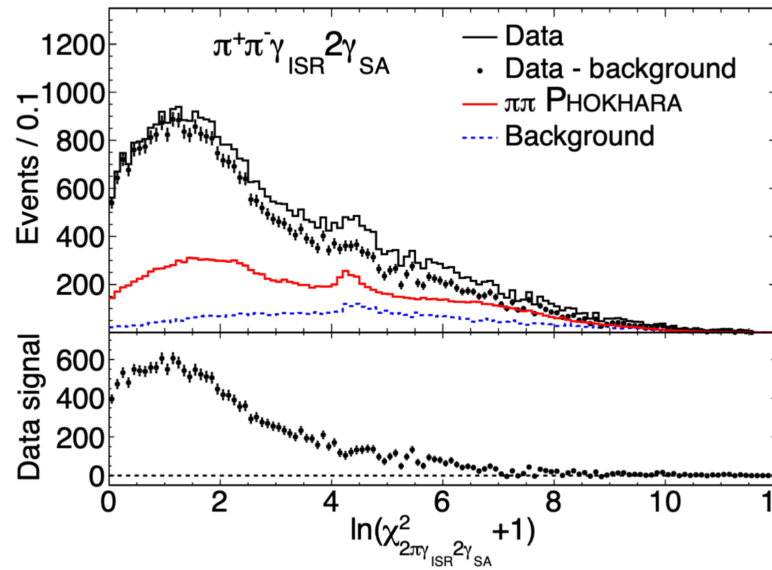

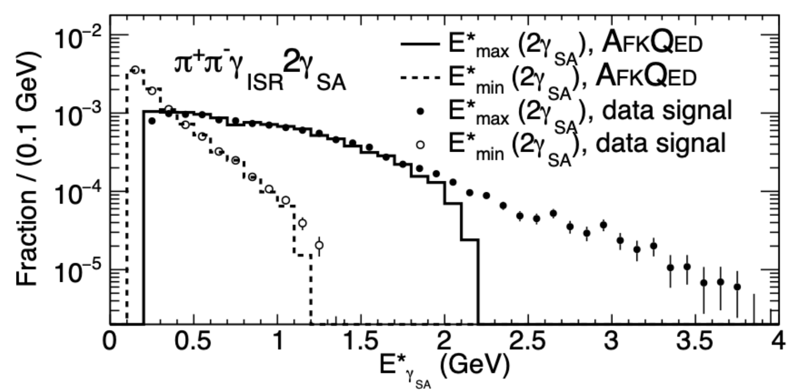

χ^2 distributions have longer tail due to collinear approximation for 2SA photons
Data/AfkQED agree in $E^*\gamma_{SA}$ shape up to 2.3 GeV

NLO background important (BDT applied for $\pi\pi$ to suppress other background)
Similar distributions $\mu\mu$ & $\pi\pi$

NNLO 1SA-1LA Fit Results ($E\gamma_{LA} > 200$MeV, $E^*\gamma_{SA} > 100$MeV)

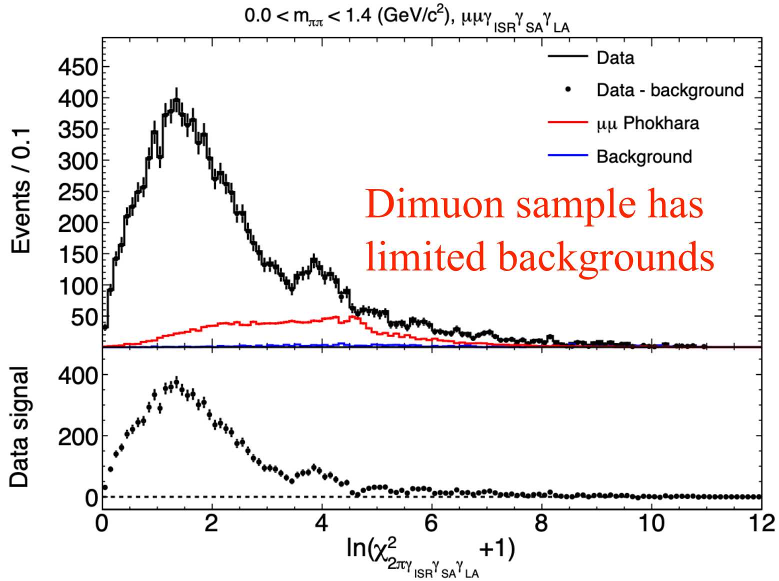

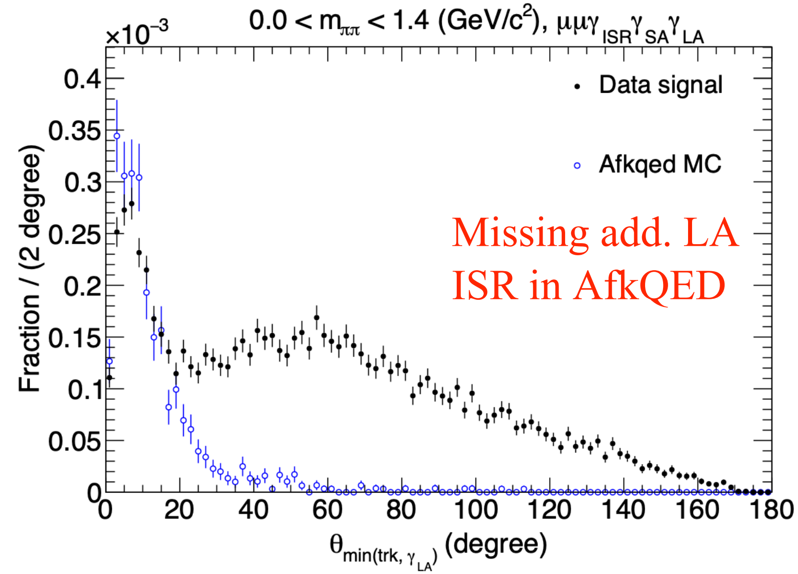

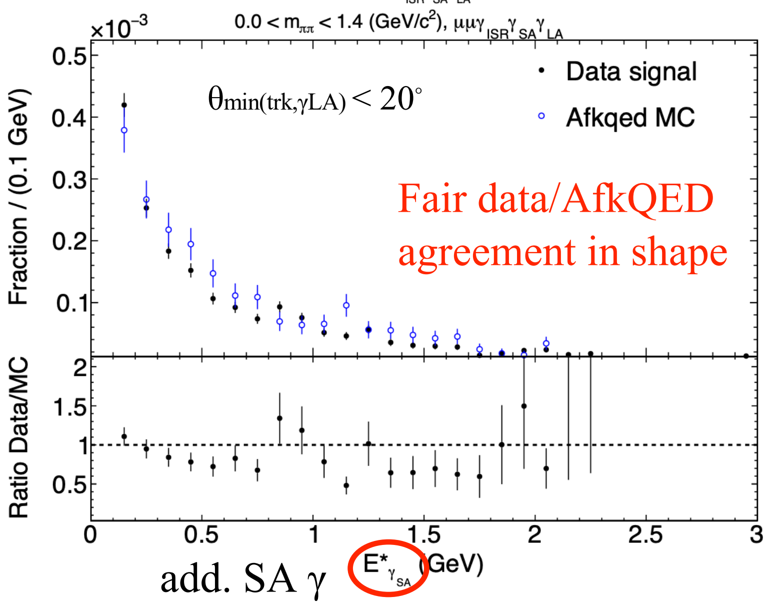

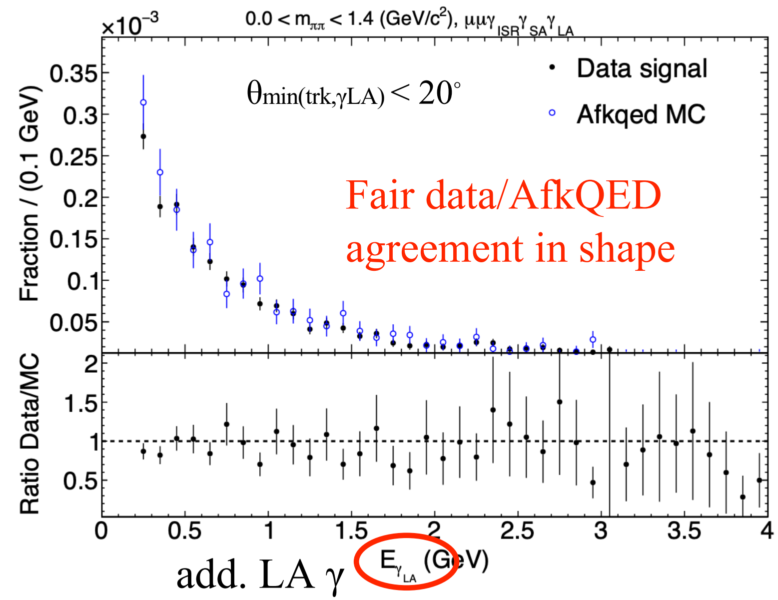

NNLO 2LA Fit Results ($E\gamma_{LA1,2} > 100$ MeV)

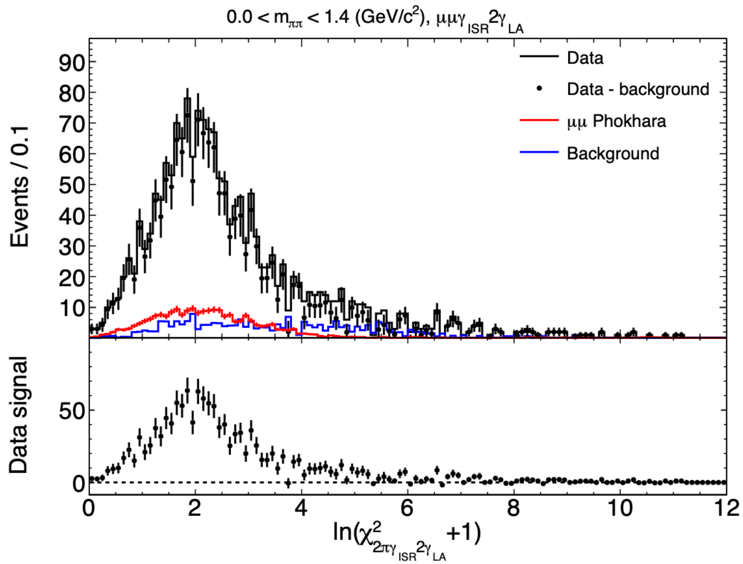

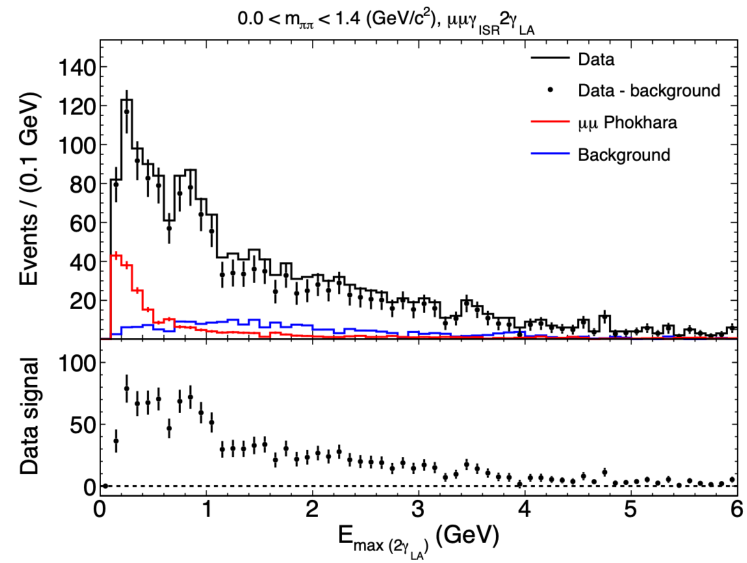

Background again small in dimuon process

Much larger background in pipi process suppressed by

- vetoing π^0 and η with 2 mass windows
- apply additional BDT selection

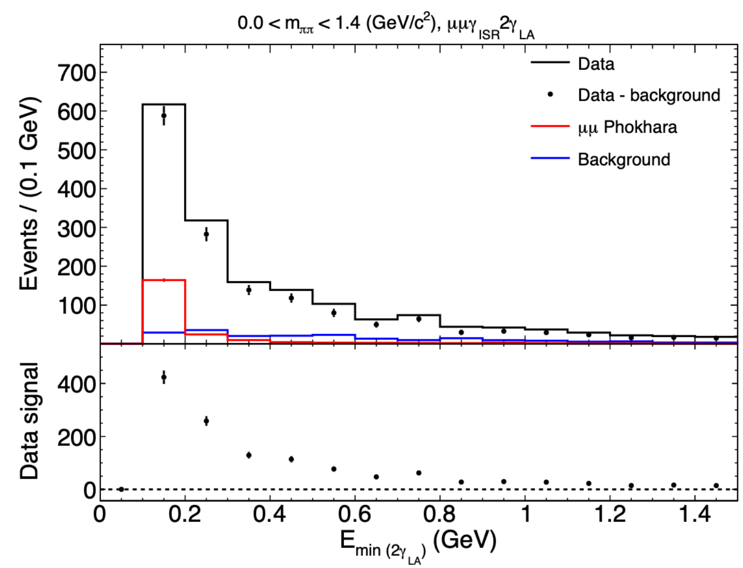

From Fitted Categories to Physical Ones

- ➢ Selection efficiency (including BDT for dipion processes)

- ➢ Feed-through corrections
  - ➢ Mostly based on MC expectations
  - ➢ With the collinear approximation, 2 SA photons from a same beam not reconstructed in NNLO category ➜ data-driven estimation
  - ➢ AfkQED $E_{add,\gamma}$ spectrum limited to 2.3 GeV ➜ data-driven estimation

- ➢ Correct data/MC difference in rate (iterative procedure)

- ➢ FSR and LA ISR separation using template fits (backup)

Efficiency and Feed-through Corrections

→ Fitted categories

↓ True categories (same energy thresholds)

%	LO	$\gamma_{\rm ISR}\gamma_{\rm SA}$	$\gamma_{\rm ISR}\gamma_{\rm LA}$ ($< 20^\circ$)	$\gamma_{\rm ISR}\gamma_{\rm LA}$ ($> 20^\circ$)	$\gamma_{\rm ISR}2\gamma_{\rm SA}$	$\gamma_{\rm ISR}\gamma_{\rm SA}\gamma_{\rm LA}$ ($< 20^\circ$)	$\gamma_{\rm ISR}\gamma_{\rm SA}\gamma_{\rm LA}$ ($> 20^\circ$)
	$\mu\mu$ ($m_{\pi\pi} < 1.4\,\mathrm{GeV/c^2}$)						
LO	**99.64(1)** **99.439(3)**	*0.223(9)* 0.289(2)	*0.008(2)* 0.0140(4)	*0.033(3)* 0.0756(9)	*0.139(7)* 0.136(1)	*0.0004(4)* 0.00011(3)	*0.005(1)* 0.0073(3)
$\gamma_{\rm ISR}\gamma_{\rm SA}$	*0.327(1)* 0.325(2)	**97.9(5)** **94.28(2)**	*0.006(1)* 0.0169(4)	*0.008(2)* 0.212(1)	*0.254(9)* 0.838(3)	*0.0021(9)* 0.0077(3)	*0.010(2)* 0.127(1)
$\gamma_{\rm ISR}\gamma_{\rm LA}$ ($< 20^\circ$)	*0.096(6)* 0.118(1)	*0.008(2)* 0.0113(3)	**74.8(8)** **78.8(1)**	*0.0017(7)* 0.0057(2)	*0.103(6)* 0.138(1)	*0.005((1)* 0.0008(1)	*0.0014(7)* 0.0007(1)
$\gamma_{\rm ISR}\gamma_{\rm LA}$ ($> 20^\circ$)	*0.003(1)* 0.099(1)	*0.0016(7)* 0.0645(8)	*0.0023(9)* 0.0045(2)	*0.181(8)* **83.89(6)**	*0.003(1)* 0.0517(7)	*0(0)* 0.00021(5)	*0.0010(6)* 0.0135(4)
$\gamma_{\rm ISR}2\gamma_{\rm SA}$	0.19(2)	1.69(3)	0.014(2)	0.003(3)	**90.8(5)**	0.0010(5)	0.0015(5)
$\gamma_{\rm ISR}\gamma_{\rm SA}\gamma_{\rm LA}$ ($< 20^\circ$)	0.010(1)	0.074(4)	0.005(1)	0.0007(5)	0.035(4)	**72.2(1.6)**	0.0004(4)
$\gamma_{\rm ISR}\gamma_{\rm SA}\gamma_{\rm LA}$ ($> 20^\circ$)	0.0007(5)	0.010(2)	0(0)	0.0013(7)	0.004(1)	0.0007(5)	*0.042(4)*
Rest	0.0011(6)	0.003(1)	0.0011(6)	0(0)	0.011(2)	0.007(2)	0.003(1)

- ➢ Diagonal numbers show selection efficiencies from AfkQED (1st row in each block) and Phokhara (2nd row)
- ➢ Non-diagonal ones show feed-through probabilities normalized to total event yields
- ➢ Data/MC difference especially in LA categories taken into account
- ➢ Pipi processes (not shown) have lower efficiencies for those categories selected with BDT

NLO Results after Removing NNLO Contribution

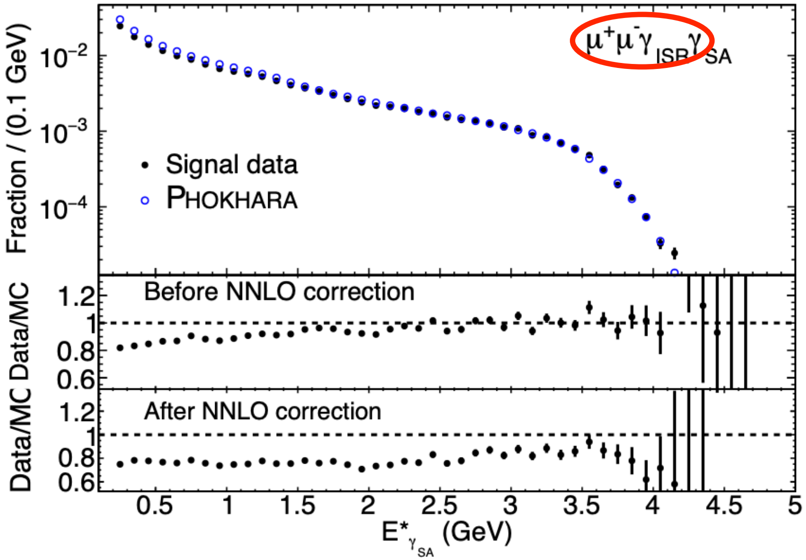

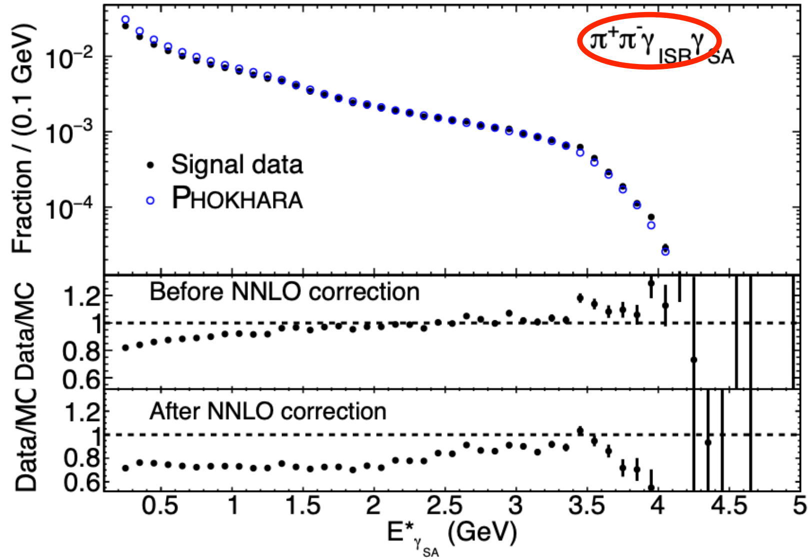

$E^*_{\gamma SA}$ data/Phokhara ratios become flatter (bottom panel) in both $\mu\mu$ & $\pi\pi$ processes
NNLO in data gives harder spectrum due to coalesced photons in collinear approximation

Phokhara excess in NLO with 2 hard photons remains after the NNLO correction

Final Results (Table I in PRL draft)

TABLE I: Event fractions in data for the $\mu\mu$ and $\pi\pi$ processes in all fit categories. The numbers in parentheses represent uncertainties, where the first is statistical and the second systematic. The results, except for NNLO 2LA (which is not simulated by any generator currently available) are corrected using efficiencies that vary category-by-category between 99% and 72%, except for NLO FSR $\pi\pi$ (40%) and NNLO FSR $\pi\pi$ (22% due to BDT selection.)

Category	$\mu\mu$ $m_{\pi\pi} < 1.4\,\mathrm{GeV}/c^2$	$\pi\pi$ $0.6 < m_{\pi\pi} < 0.9\,\mathrm{GeV}/c^2$
LO	0.7716(4)(14)	0.7839(5)(12)
NLO SA-ISR	0.1469(3)(36)	0.1401(2)(16)
NLO LA-ISR	0.0340(2)(9)	0.0338(2)(9)
NLO ISR	0.1809(4)(35)	0.1739(3)(20)
NLO FSR	0.0137(2)(7)	0.0100(1)(16)
NNLO ISR [a]	0.0309(2)(38)	0.0310(2)(39)
NNLO FSR [b]	0.00275(6)(9)	0.00194(12)(50)
NNLO 2LA [c]	0.00103(3)(1)	0.00066(4)(4)

[a] NNLO ISR = 2SA-ISR or SA-ISR + LA-ISR
[b] NNLO FSR = SA-ISR + LA-FSR
[c] NNLO 2LA = 2LA-ISR, LA-ISR + LA-FSR or 2LA-FSR

Systematic uncertainties include those from efficiency corrections, background subtraction and feed-through corrections with the latter two being the dominant contributions

Summary of Publication 1

- NNLO radiation with three photons observed for the first time with a fraction of (3.47 ± 0.38)% for muons and (3.36 ± 0.39)% for pions
  - This allows to remove NNLO feed-through contributions from NLO
  - The resulting shape of the SA γ energy provides good internal consistency
- Phokhara NLO SA γ fraction is higher than data with data/MC ratios of 0.763 ± 0.019 for dimuons and 0.750 ± 0.008 for pipi, while the respective LA ISR ratios, 0.96 ± 0.03 and 0.98 ± 0.03, are consistent with unity
  - This indicates a problem in the angular distribution of the 2 hard-photon rate generated by Phokhara, with a large excess at small angles to the beams
- AfkQED MC provides a reasonable description of the rates and energy distributions of NLO and NNLO data up to the cutoff at 2.3 GeV photon energy, with slightly high (SA+LA)-ISR NLO data/MC ratios of 1.060 ± 0.015 for muons and 1.043 ± 0.010 for pions
- The ratio between data and the Phokhara prediction for FSR NLO is found to be 0.86 ± 0.05 for muons and 0.76 ± 0.12 for pions. The corresponding data/AfkQED ratios are 1.10 ± 0.06 for muons and 1.08 ± 0.10 for pions. In both cases, the ratio pion/muon is consistent with one and supports the pion point-like behavior for additional FSR.
  - This result, that includes a data/MC correction for fake photon subtraction and takes into account NNLO feed-through, supersedes the previous result of an excess of (21 ± 5)% observed in the previous BABAR analysis

Main Results of Publication 2

- Did a new combination including the new CMD-3 $\pi\pi$ measurement to quantify the tension among different $\pi\pi$ measurements
- Studied possible consequences of BABAR's hard photon findings on KLOE and BESIII measurements
- New landscape of HVP evaluations

New Combination

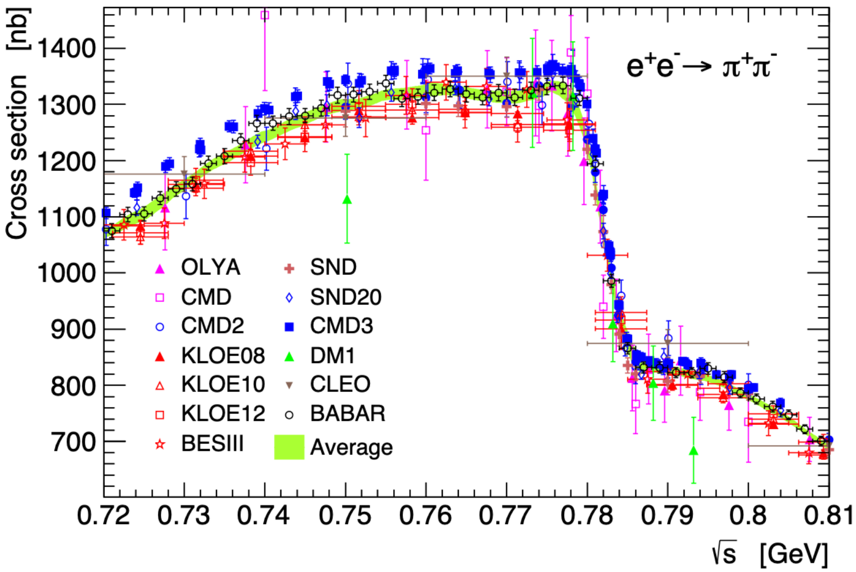

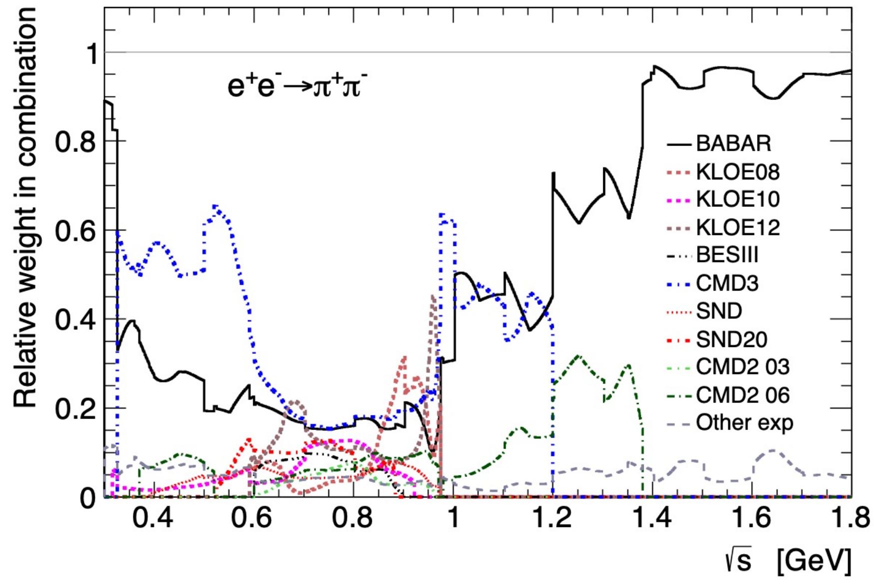

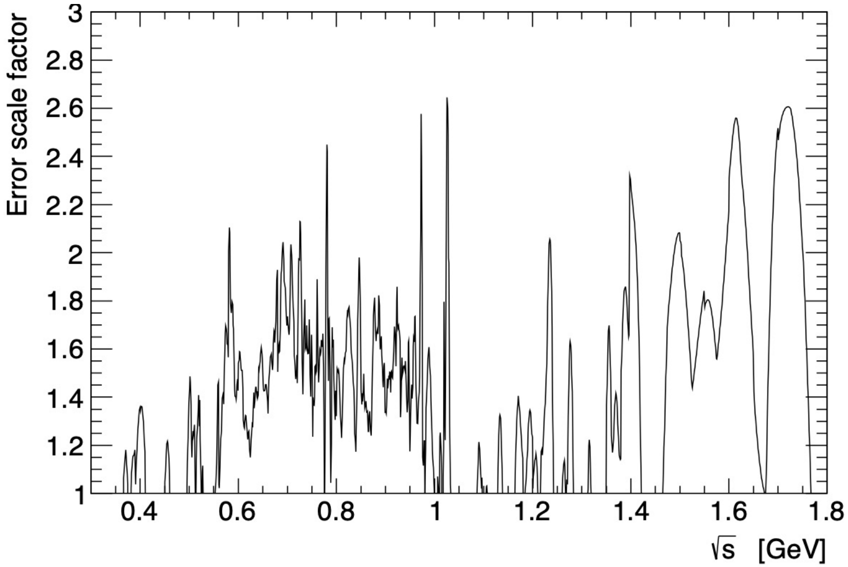

Top-left: different densities and scales of the measurements

Top-right: relative weight of each experiment

Bottom-left: local χ^2 per degree of freedom

Tention/Discrepancies Among 3 Most Precise Datasets

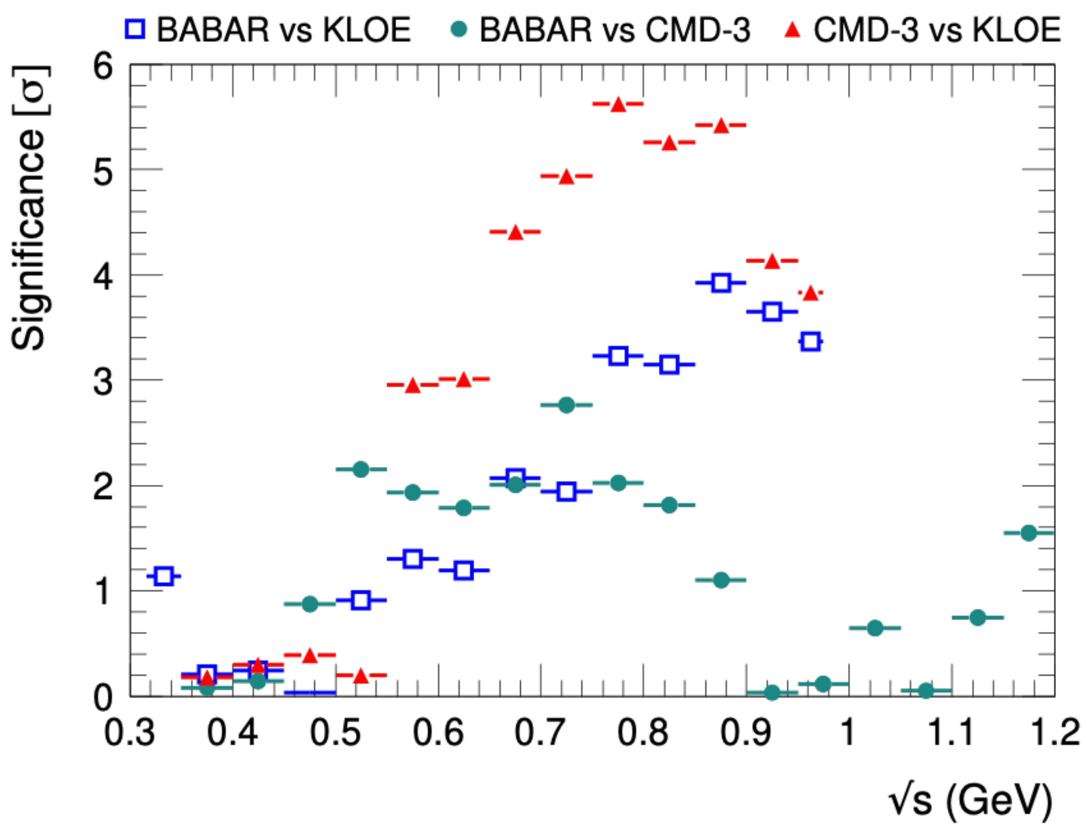

Discrepancy between CMD-3 and KLOE over 5σ in the ρ mass peak region!

BABAR and CMD-3 in better agreement, below 3σ

Possible Consequences of Using Phokhara: KLOE

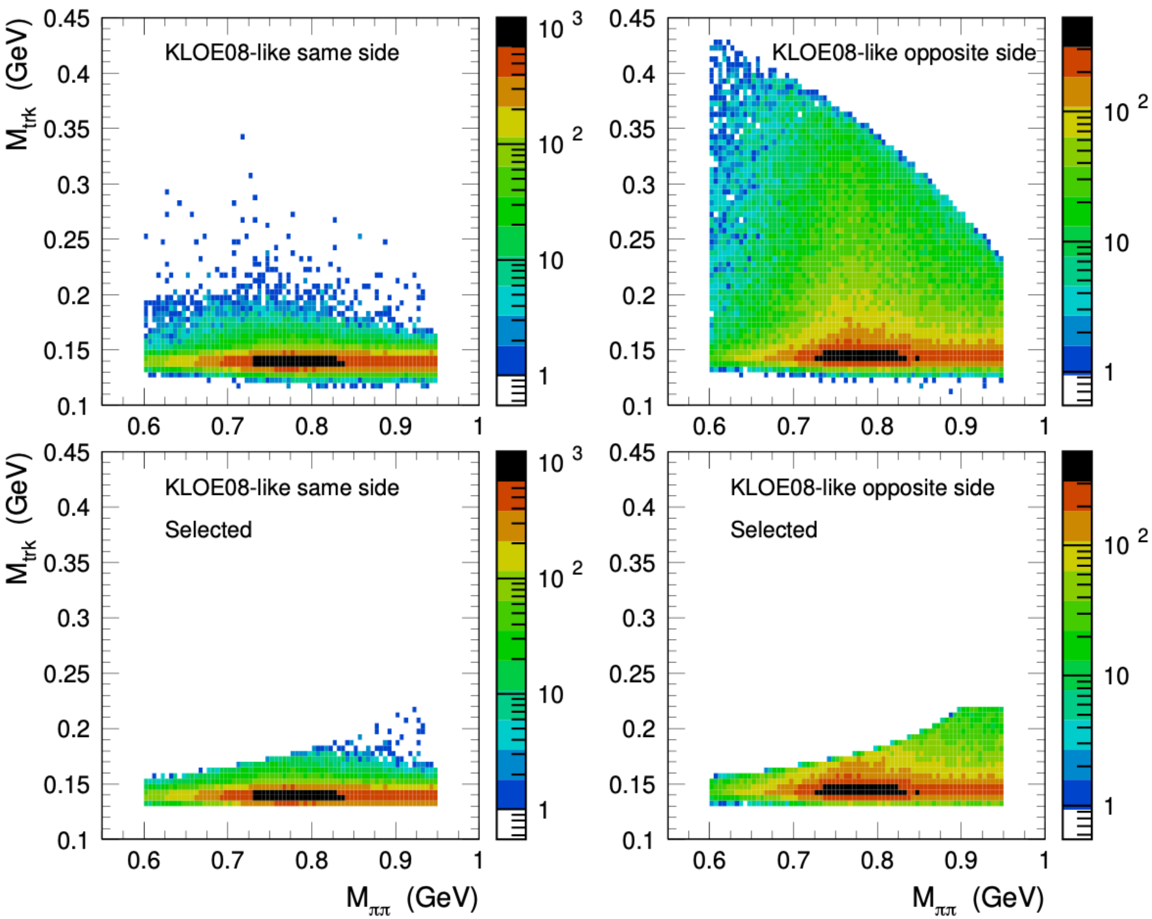

KLOE uses a Mtrk variable to select/separate $\pi\pi$ and $\mu\mu$ events

When there is a 2nd hard photon opposite to the 1st one, the selection efficiency is affected

This effect was not fully taken into account in the measurement due to the deficiencies of the Phokhara MC sample used

Quoted systematic uncertainty of 0.5% for missing higher orders is underestimated

Possible Consequences of Using Phokhara: BESIII

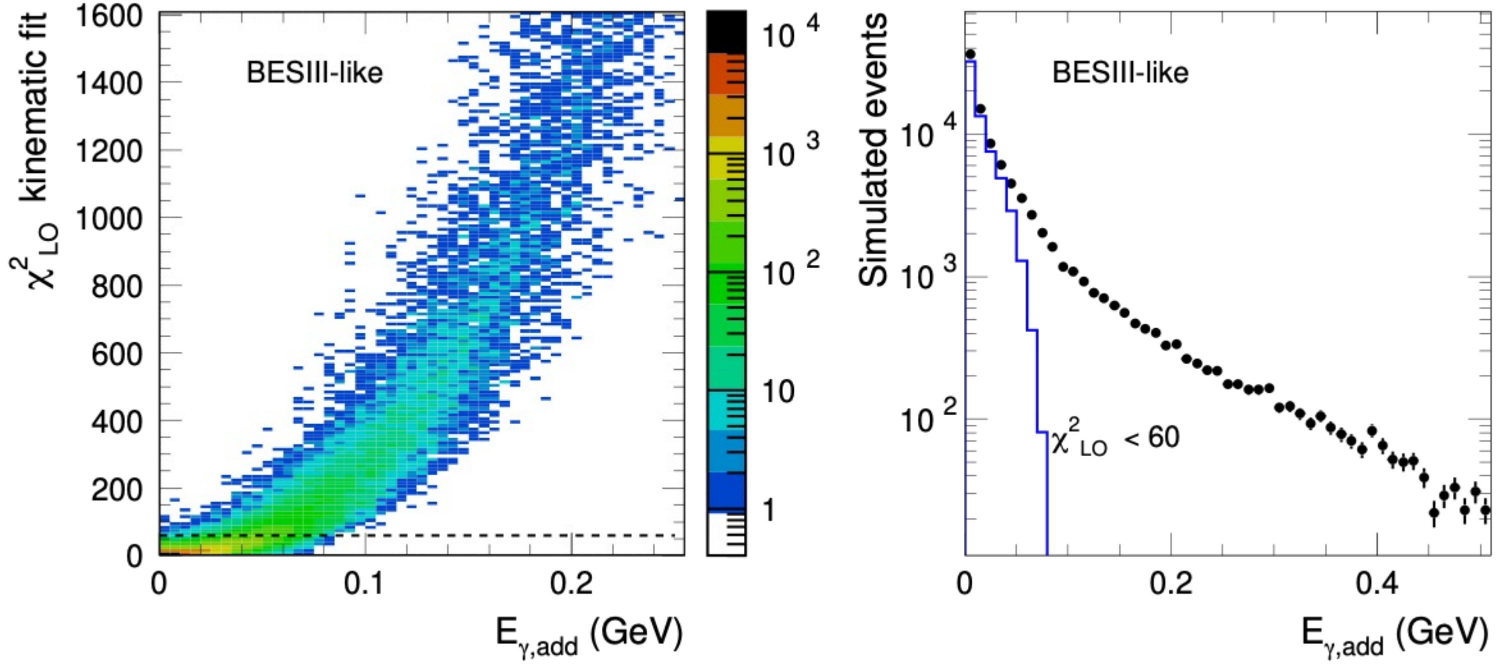

Similarly for BESIII, events with an additional hard photon have a bad χ^2 fit
They are lost with the χ^2 selection
Again, the quoted uncertainty of 0.5% for missing higher orders underestimated

New Landscape of the HVP Evaluations

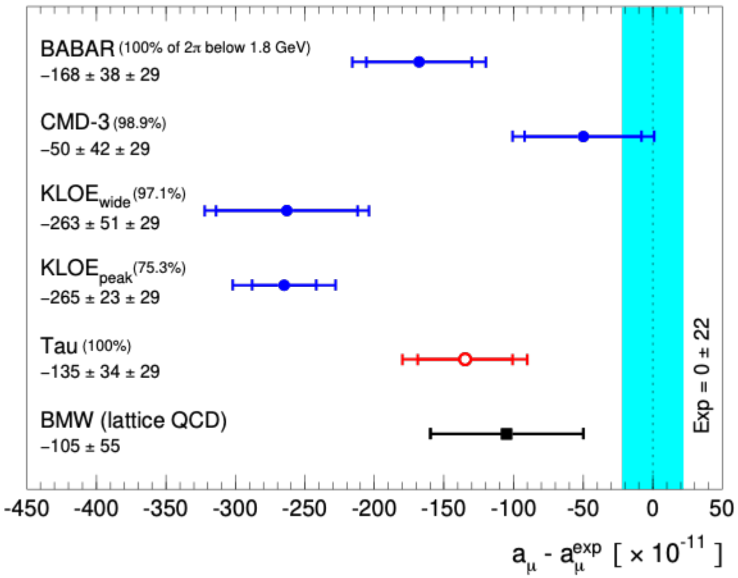

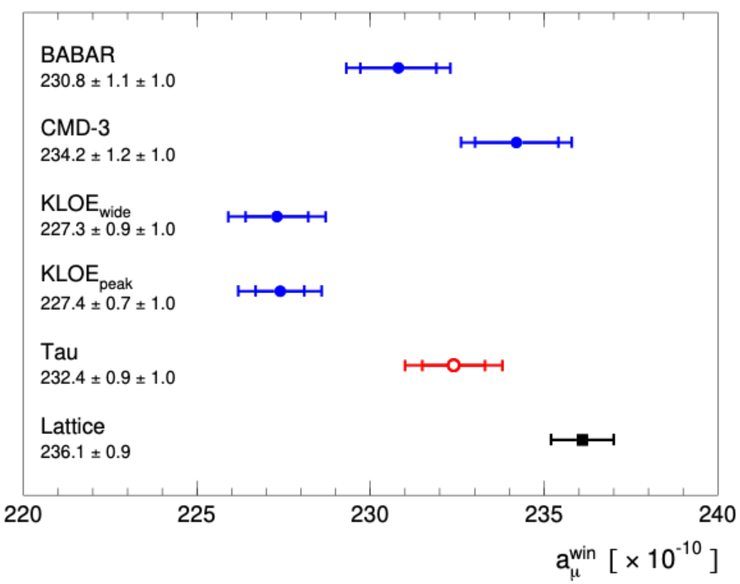

Calculate HVP a_μ ou a_μ^{win} for each experiment/dataset by including missing part using the combined data

- ➢ BABAR, CMD-3, tau data are in fair agreement
- ➢ They are also in agreement with BMW (lattice QCD) based prediction
- ➢ The predictions are closer to the measurement (vertical blue band) if excluding KLOE data

- ➢ Similar conclusion for a_μ^{win} though the spread is larger between different experiment/dataset

Summary for Both Publications

- ➢ The discrepancy between BABAR and KLOE could be partly due to the deficiencies of the used Phokhara MC samples
  - ➢ It is important to use a better MC sample including higher order radiation, e.g. KKMC
- ➢ It is important to have precise and independent measurements to resolve the BABAR, CMD-3 and KLOE discrepancies
- ➢ Without resolving the discrepancy, the dispersion-relation-based HVP prediction cannot be improved further, while the measurement from Fermilab is already more precise
- ➢ We also need to understand the difference with lattice-based prediction [we have an ANR project (HVP4NewPhys) ongoing with lattice people from Marseille]
- ➢ Belle II can play a key role here by measuring $\tau\to\pi\pi^0\nu_\tau$ mass spectrum [Flavien] and $e^+e^-\to\pi^+\pi^-$ cross section [Kylian]

Additional Slides

- ➢ Comparison Phokhara and AfkQED
- ➢ FSR and LA ISR separation
- ➢ Bias studies of the collinear approximation in the NLO SA fit
- ➢ Fake photon and photon efficiency studies
- ➢ Feed-through corrections
- ➢ Comparison of angular resolution data/MC
- ➢ 2D-χ^2 distributions for NNLO signal events

Phokhara vs AfkQED

	Phokhara 9.1 [1]	AfkQED [2]
Lowest order ISR process	$\pi\pi\gamma$ / $\mu\mu\gamma$	
NLO: Additional ISR	Full matrix element	Collinear to e+ or e− beam [3] ($mx_\gamma > 8$ GeV/c^2 $\rightarrow$ $E_\gamma < 2.3$ GeV)
FSR:	idem	Photos [4]
NNLO Additional ISR		idem ISR NLO

[1] JHEP 02 (2014) 114

[2] PLB 459 (1999) 279; EPJC 18 (2001) 497

[3] Structure function method, Nuovo Cim. A110 (1997) 515

[4] Comput. Phys. Comm. 66 (1991) 115

FSR and Additional LA ISR Separation

It is possible to separate statistically FSR from additional LA ISR γ
using
- FSR template from AfkQED and
- LA ISR template from Phokhara−AfkQED FSR

then do a template fit

The same technique is applied later in the NNLO categories

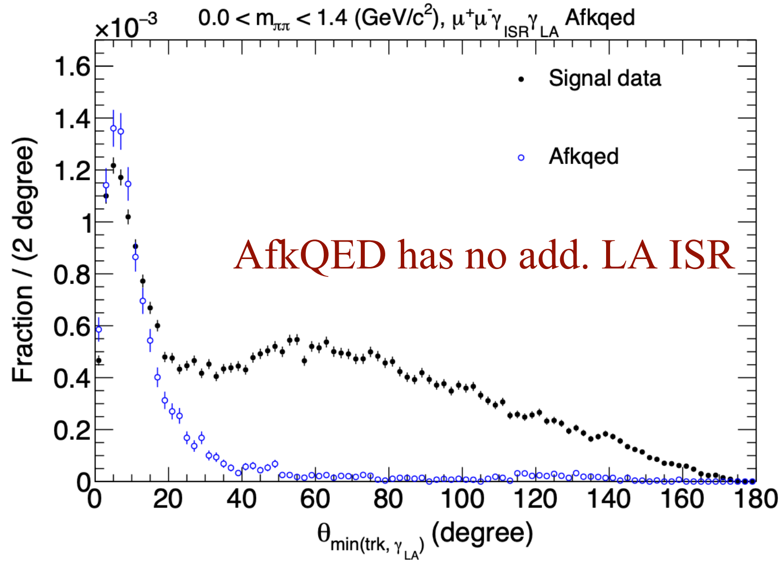

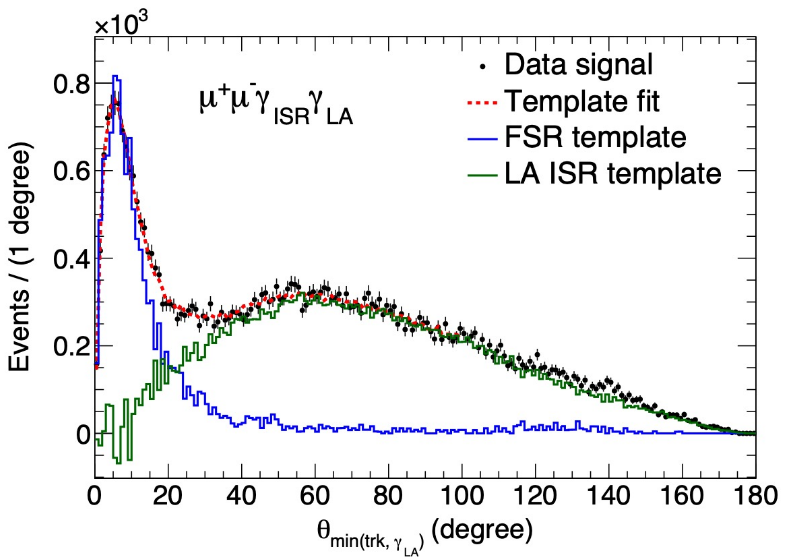

Bias studies of Collinear Approximation

The collinear approximation in the SA fit introduced two biases:

- long tail in the is χ^2 distribution for more central and larger energy ISR γ
- the energy of the additional photon towards smaller energy for ISR γ away from the beam direction

The biases are studied with MC and checked with data in the latter case

Impact of Collinear Approximation on χ^2

The long tail in the SA χ^2 distribution is checked with MC to be due to the collinear approximation: More central and larger energy ISR γ has longer tail

Similar bias expected in data

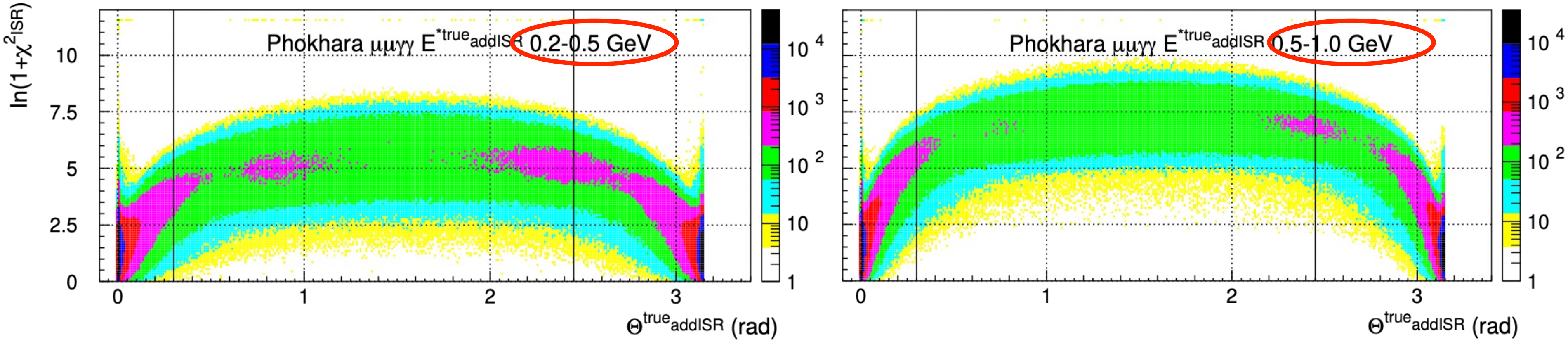

Impact of Collinear Approximation on $E^*_{\gamma SA}$

The bias on the fitted SA γ CM energy is checked using LA γ CM energy as reference

For γ near the detector acceptance edges, the bias is found smaller than more central γ

For γ outside of the detector acceptance near the beam direction, the bias is expected to be smaller

The bias is well simulated by MC

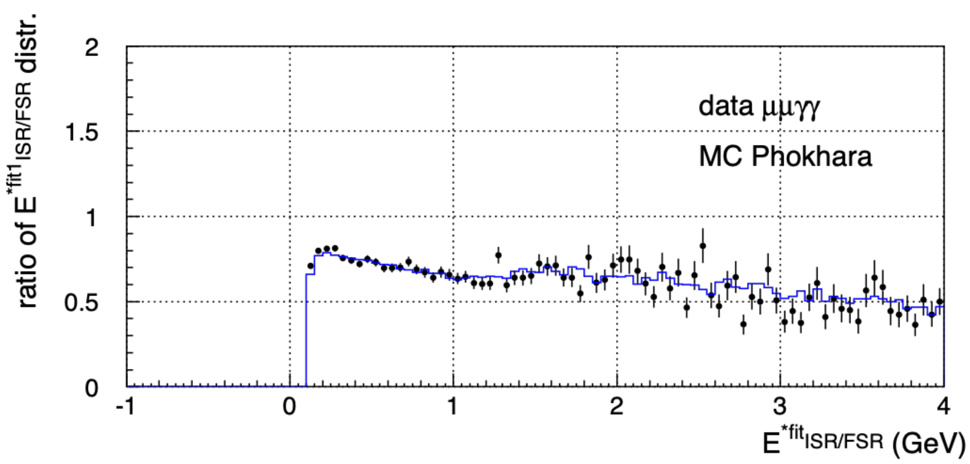

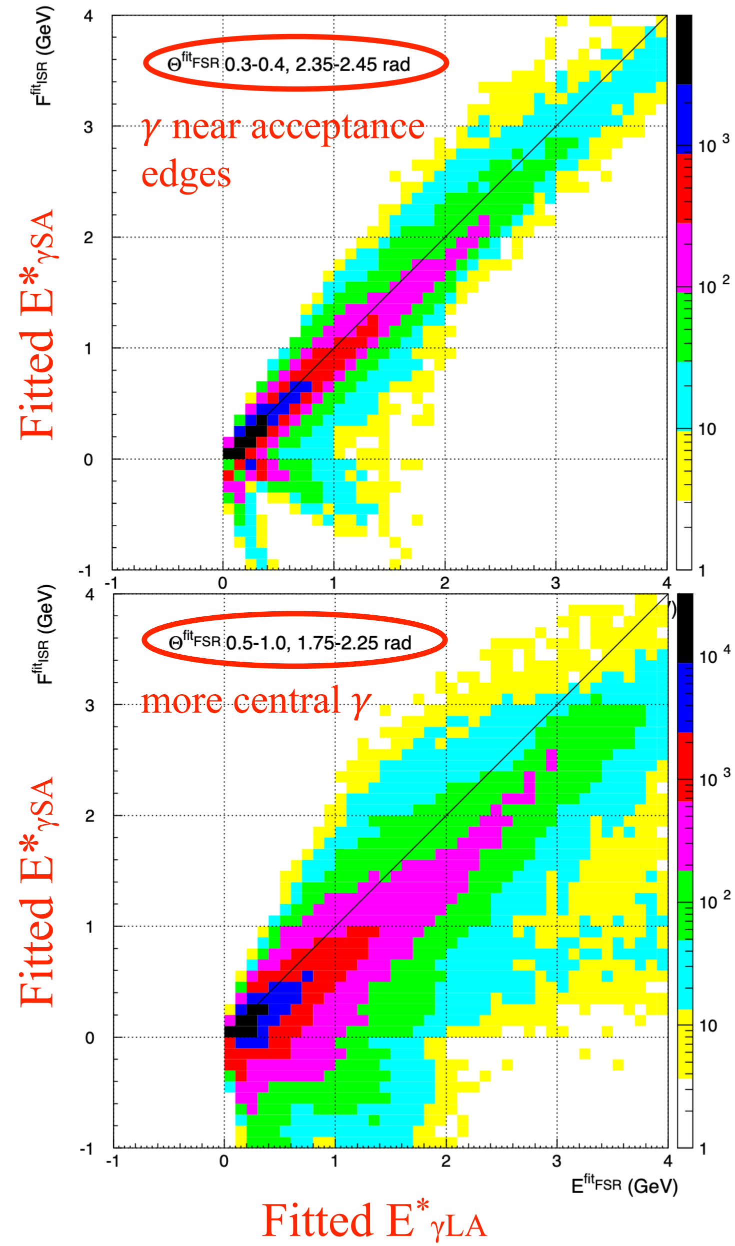

Fake Photon and Photon efficiency Studies

- ➢ Fake photon correction in the dipion processes (new wrt to the old analyses)
- ➢ Additional LA photon efficiency evaluation

Fake Photon Contribution In Dipion Processes (1)

Fake photon contribution due to shower fluctuation near a pion track is studied using energy deposition and Zernike20 (transverse shower shape) parameter in EM calo

Four regions are defined to probe different fake photon contributions as shown in $\theta_{min(trk,\gamma LA)}$ distribution (data/Phokhara normalized at $40^{\circ}-100^{\circ}$)

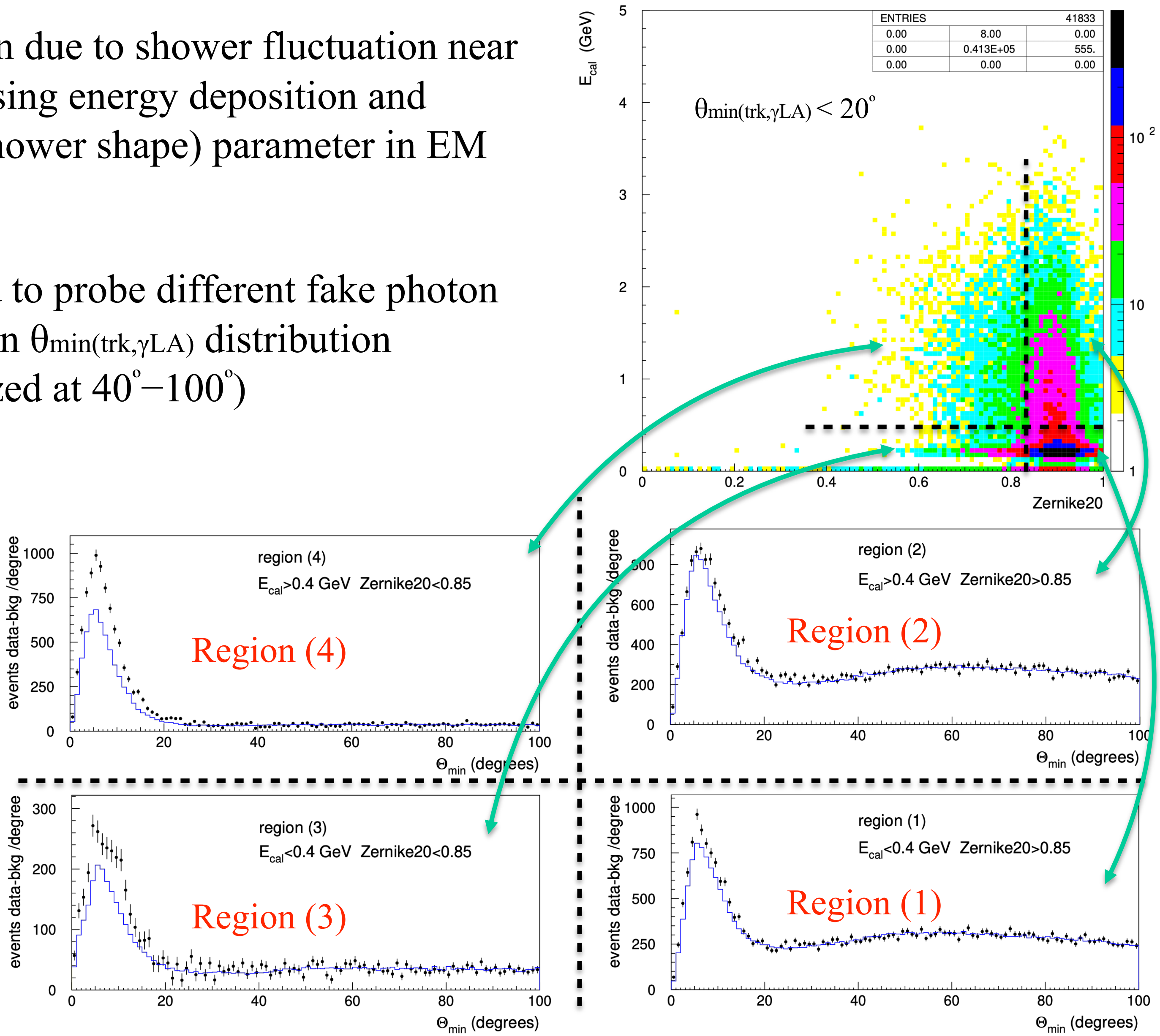

Fake Photon Contribution In Dipion Processes (2)

Template fits performed in χ^2 distributions in each of four regions using:

- FSR γ template from LA ISR γ $\theta_{min(trk,\gamma LA)} > 20^{\circ}$
- Fake γ template from region (4)

Two examples of the fits in regions (2) and (3) are shown comparing data (left) and Phokhara (right)

Fake fraction results:
Data: $0.458 \pm 0.004_{stat} \pm 0.010_{sys}$
Phok: $0.377 \pm 0.004_{stat} \pm 0.007_{sys}$

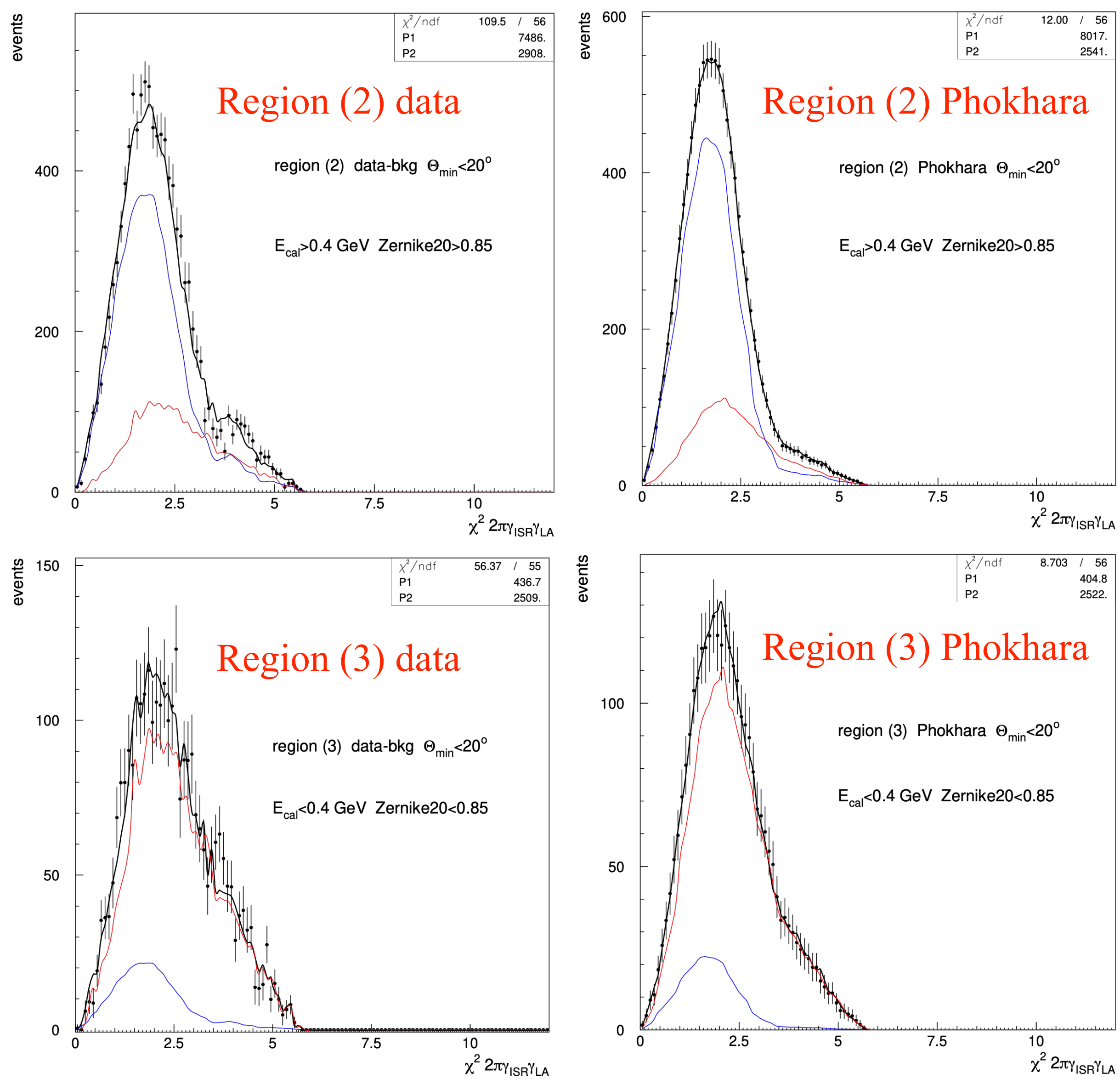

Additional LA Photon Efficiency Study (1)

Additional LA γ efficiency study performed using $2\pi\pi^0\gamma$

A dedicated kinematic fit performed to obtain the $2\pi\pi^0\gamma$ samples by constraining two additional photons to π^0

Background from $\pi\pi\gamma\gamma$ and $\mu\mu\gamma\gamma$ processes is removed by χ^2 selection

The mass distribution $2\pi\pi^0\gamma$ shows the dominance of ω and φ resonances, background subtracted using MC simulation is dominated by $2\pi2\pi^0\gamma$

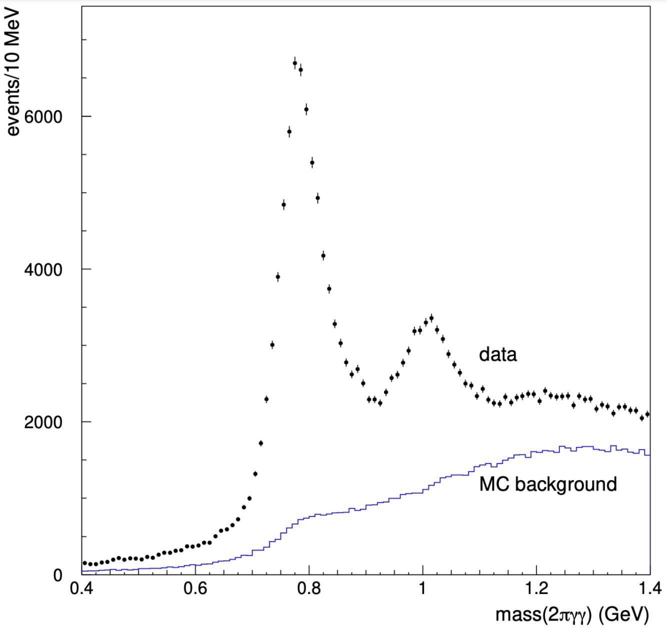

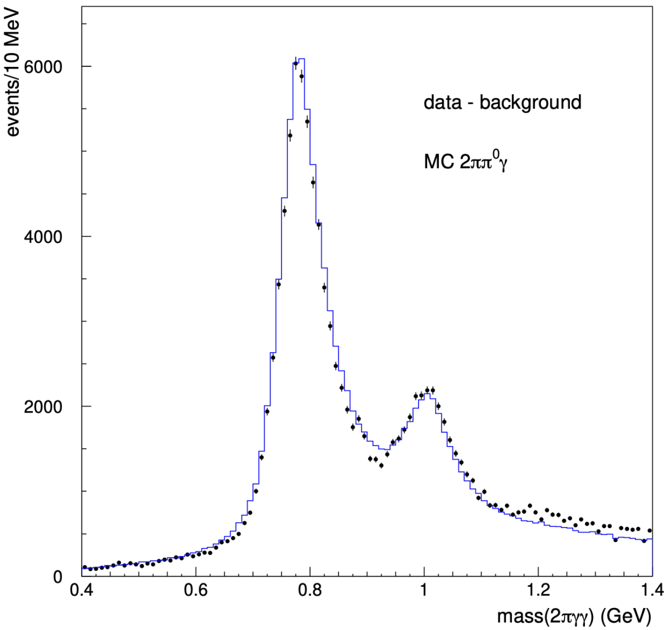

Additional LA Photon Efficiency Study (2)

The efficiency is obtained by matching one measured photon with the expected one from π^0 in three 3 θ regions, one of which 0.35−0.45 rad is shown here as an example

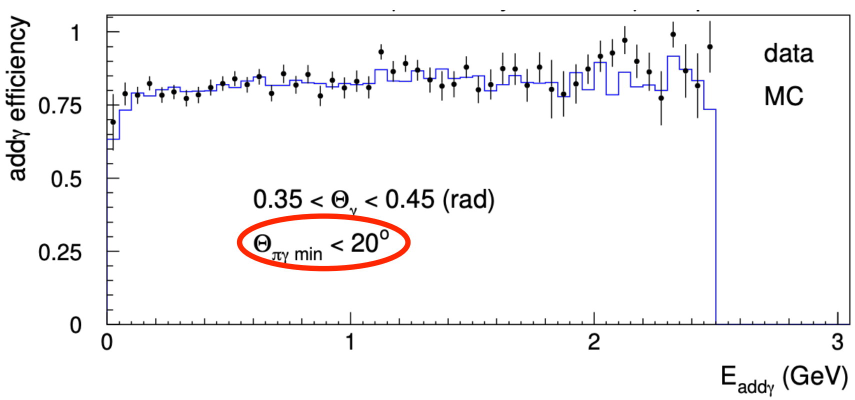

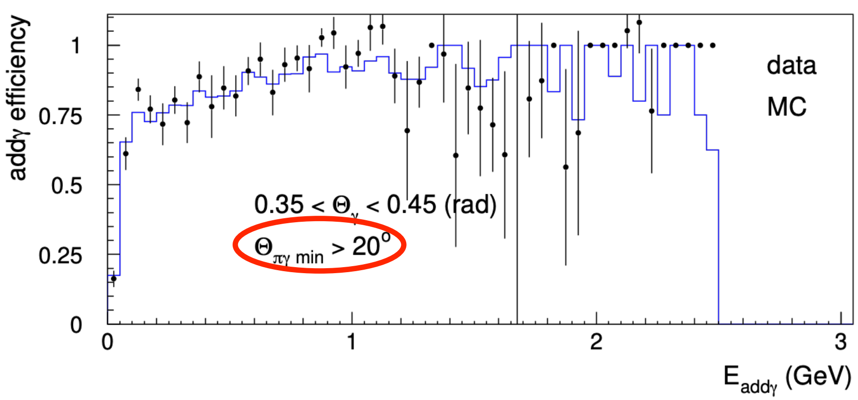

The efficiency is also shown as a function of $\theta_{min(\pi,\gamma)}$. Data/MC agrees within 2%

→ no efficiency correction is applied

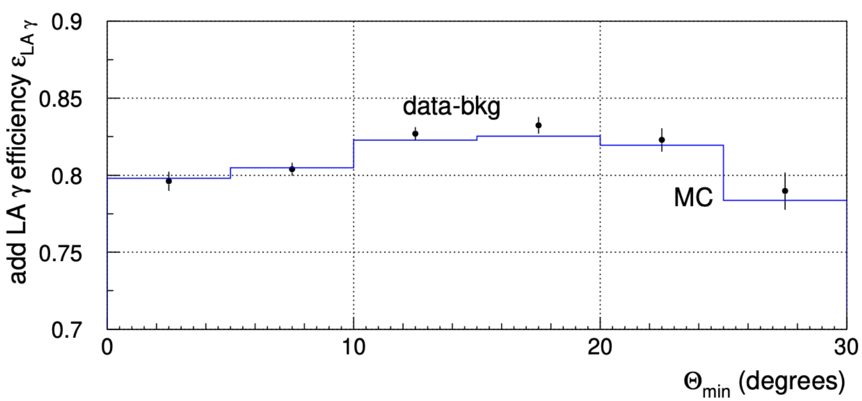

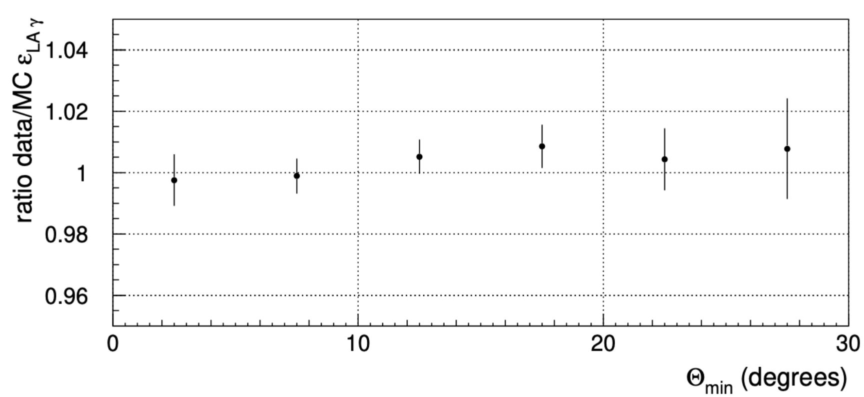

Feed-through Correction

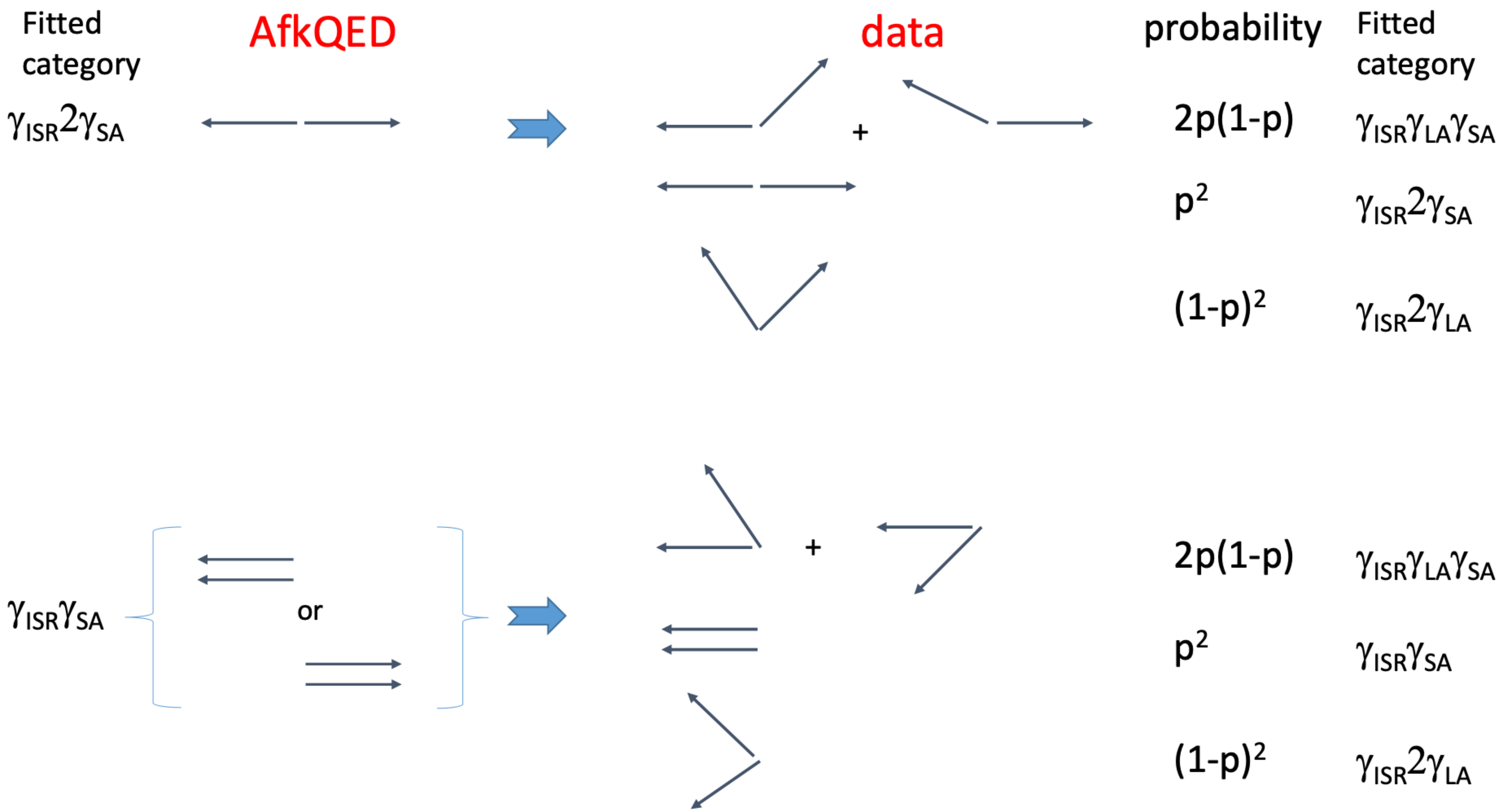

Comparison of angular resolution data/MC

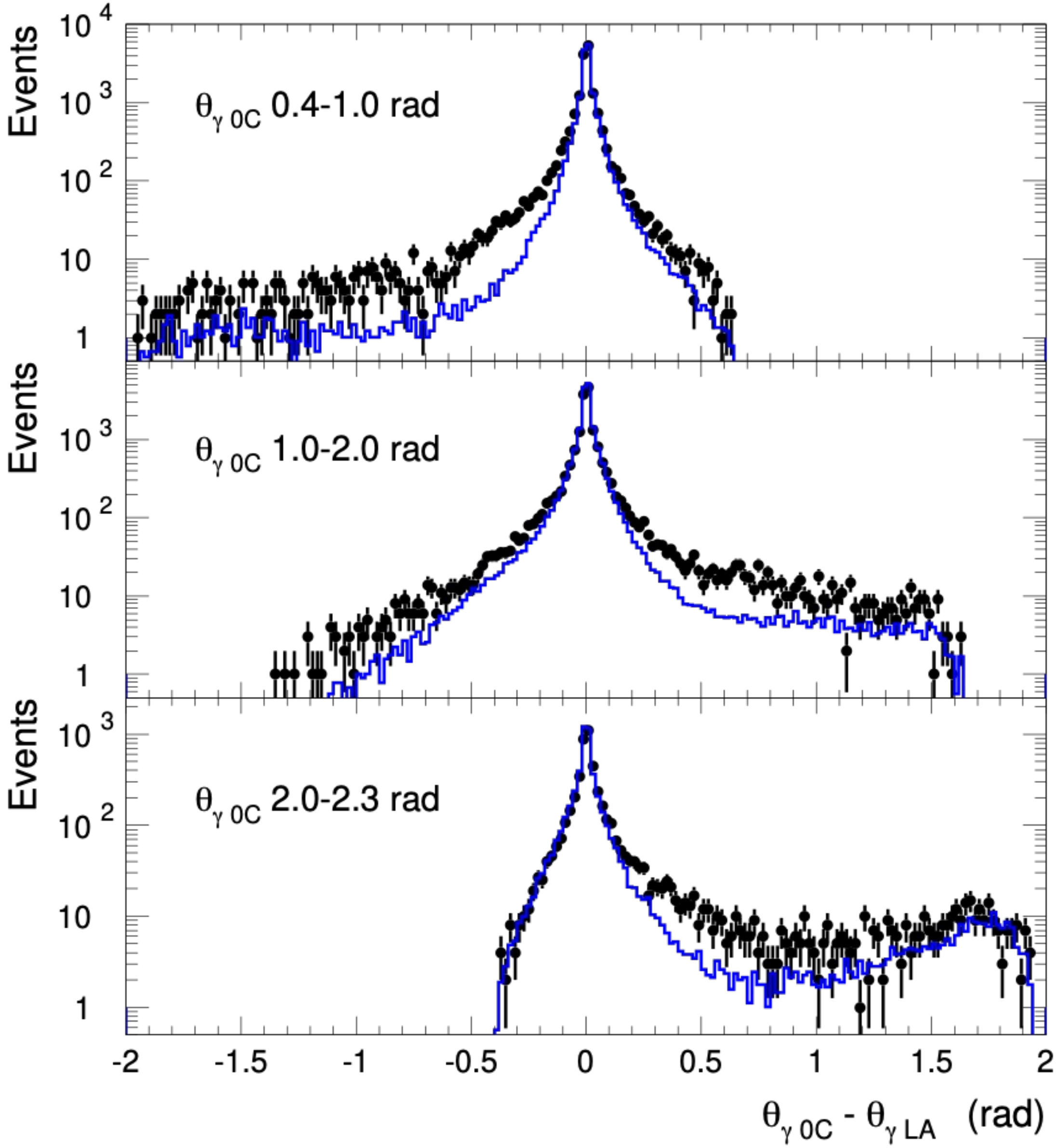

In the bulk phase space, the data resolution is well simulated.

Only in the tails, the angular resolution in data is slightly worse.

This implies that the data/Phokhara deficit at small angles in the 0C calculation is unlikely due to detector resolution effects

2D-χ^2 distributions for NNLO Signal Events

NNLO 2SA signals

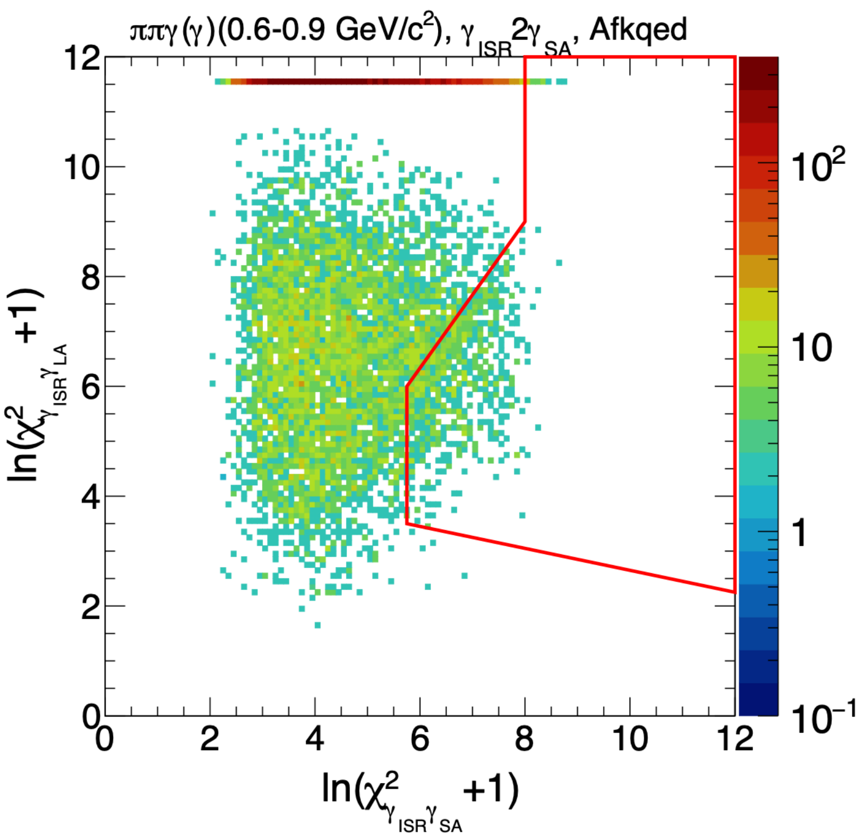

NNLO SA+LA signals

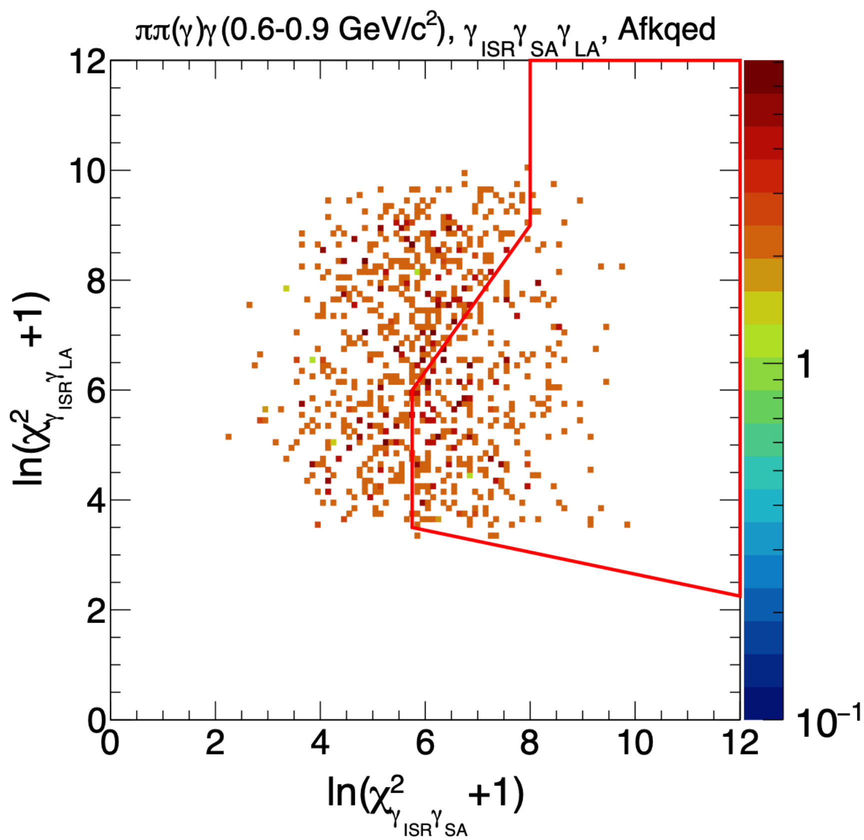

NNLO signals are partially distributed in the 2D-χ^2 rejected region

→ No 2D-χ^2 selection applied for the NNLO analysis